INVESTIGATION OF THE EFFECT OF ALLOYING ELEMENTS ON MARTENSITIC TRANSFORMATION IN C-Mn STEELS BY COMPUTATIONAL MATERIALS ENGINEERING TECHNIQUES

A THESIS SUBMITTED TO
THE GRADUATE SCHOOL OF NATURAL AND APPLIED SCIENCES
OF
MIDDLE EAST TECHNICAL UNIVERSITY

BY

FATİH AKSU

IN PARTIAL FULFILLMENT OF THE REQUIREMENTS
FOR
THE DEGREE OF MASTER OF SCIENCE
IN
METALLURGICAL AND MATERIALS ENGINEERING

APRIL 2024

Approval of the thesis:

INVESTIGATION OF THE EFFECT OF ALLOYING ELEMENTS ON MARTENSITIC TRANSFORMATION IN C-Mn STEELS BY COMPUTATIONAL MATERIALS ENGINEERING TECHNIQUES

submitted by **FATİH AKSU** in partial fulfillment of the requirements for the degree of **Master of Science** i**n Metallurgical and Materials Engineering, Middle East Technical University** by,

Prof. Dr. Naci Emre Altun
Dean, **Graduate School of Natural and Applied Sciences** _____

Prof. Dr. Ali Kalkanlı
Head of the Department, **Metallurgical and Materials Eng.** _____

Assoc. Prof. Dr. Caner Şimşir
Supervisor, **Metallurgical and Materials Eng., METU** _____

Prof. Dr. Bilgehan Ögel
Co-Supervisor, **Metallurgical and Materials Eng., METU** _____

Examining Committee Members:

Prof. Dr. Cemil Hakan Gür
Metallurgical and Materials Eng, METU _____

Assoc. Prof. Dr. Caner Şimşir
Metallurgical and Materials Eng, METU _____

Assoc. Prof. Dr. Batur Ercan
Metallurgical and Materials Eng, METU _____

Assoc. Prof. Dr. Ersoy Erişir
Metallurgical and Materials Eng., Kocaeli University _____

Assist. Prof. Dr. Kemal Davut
Metallurgical and Materials Eng., IZTECH _____

Date: 19.04.2024

I hereby declare that all information in this document has been obtained and presented in accordance with academic rules and ethical conduct. I also declare that, as required by these rules and conduct, I have fully cited and referenced all material and results that are not original to this work.

Name Last name : Fatih Aksu

Signature :

ABSTRACT

INVESTIGATION OF THE EFFECT OF ALLOYING ELEMENTS ON MARTENSITIC TRANSFORMATION IN C-Mn STEELS BY COMPUTATIONAL MATERIALS ENGINEERING TECHNIQUES

Aksu, Fatih
Master of Science, Metallurgical and Materials Engineering
Supervisor: Assoc. Prof. Dr. Caner Şimşir
Co-Supervisor: Prof. Dr. Bilgehan Ögel

April 2024, 63 pages

Hadfield steel is used in the production of various products operating under impact loads and friction conditions due to its high toughness and wear resistance properties. What gives this steel its high toughness feature is that it has a metastable austenite phase at room temperature. In addition, the transformation of the metastable austenite phase on the surface to martensite due to deformation under impact provides superior wear resistance. In this study, the effect of certain alloying elements on critical martensitic transformation temperatures and stacking fault energy is examined using computational materials engineering tools. Accordingly, stacking fault energy (SFE), martensitic transformation temperatures (Ms and Md(50/30)), T-Zero temperatures are calculated and examined using JMatPro and Thermo-Calc software. Using the data obtained from the calculations, the linear regression methods are used to model the relationship between the variables and sensitivity analysis is performed. It has been observed that alloying elements are effective on SFE, martensitic transformation temperatures and T-Zero temperature.

Keywords: Hadfield Steels, Martensitic Transformation, Stacking Fault Energy, Sensitivity Analysis, Computational Materials Engineering

ÖZ

C-Mn ÇELİKLERİNDE ALAŞIM ELEMENTLERİNİN MARTENSİTİK DÖNÜŞÜM ÜZERİNDEKİ ETKİSİNİN HESAPLAMALI MALZEME MÜHENDİSLİĞİ TEKNİKLERİ İLE İNCELENMESİ

Aksu, Fatih
Yüksek Lisans, Metalurji ve Malzeme Mühendisliği
Tez Yöneticisi: Doç. Dr. Caner Şimşir
Ortak Tez Yöneticisi: Prof. Dr. Bilgehan Ögel

Nisan 2024, 63 sayfa

Hadfield çeliği, yüksek tokluk ve aşınma direnci özelliklerinden dolayı darbe yükleri ve sürtünme koşulları altında çalışan çeşitli ürünlerin üretiminde kullanılmaktadır. Bu çeliğe yüksek tokluk özelliğini kazandıran oda sıcaklığında yarı kararlı ostenit fazına sahip olmasıdır. Ayrıca yüzeydeki yarı kararlı östenit fazının darbe altında deformasyon nedeniyle martenzite dönüşmesi üstün aşınma direnci sağlar. Bu çalışmada bazı alaşım elementlerinin kritik martensitik dönüşüm sıcaklıklarına ve istifleme hatası enerjisine etkisi hesaplamalı malzeme mühendisliği araçları kullanılarak incelenmiştir. Buna göre istifleme hatası enerjisi (SFE), martensitik dönüşüm sıcaklıkları (Ms ve Md(50/30)), T-Sıfır sıcaklıkları JMatPro ve Thermo-Calc yazılımları kullanılarak hesaplanmış ve incelenmiştir. Hesaplamalardan elde edilen veriler kullanılarak değişkenler arasındaki ilişkinin modellenmesinde lineer regresyon yöntemleri kullanılmış ve hassasiyet analizi yapılmıştır. Alaşım elementlerinin SFE, martensitik dönüşüm sıcaklıkları ve T-Sıfır sıcaklığı üzerinde etkili olduğu görülmüştür.

Anahtar Kelimeler: Hadfield Çelikleri, Martensitik Dönüşüm, İstifleme Hatası Enerjisi, Hassasiyet Analizi, Hesaplamalı Malzeme Mühendisliği

To my family…

ACKNOWLEDGMENTS

First of all, I would like to express my deepest gratitude to my supervisor Assoc. Prof. Dr. Caner Şimşir for his guidance, advice, criticism, encouragements and insight throughout my thesis study.

I would also like to offer my special thanks to my co-supervisor Prof. Dr. Bilgehan Ögel for his support.

I would like to thank ONATUS Öngörü Teknolojileri for allowing the usage of JMatPro® and Thermocalc® software.

I would like to thank PINAR DÖKÜM for material supply and help to this work.

I am also grateful to my friends for their support.

I would like to give special thanks to my family; my beloved wife Ayşenur Aksu, my dear mother and father Elif Aksu and Murat Aksu, and my dear brother Bekir Aksu. Without the love, faith, and support of my wife and family, I could not have made it through this whole period.

TABLE OF CONTENTS

LIST OF TABLES

TABLES

LIST OF FIGURES

FIGURES

LIST OF ABBREVIATIONS

ABBREVIATIONS

CALPHAD: Calculation of phase diagrams

Ms: Martensite start temperature

Md: Upper limit temperature of deformation induced martensitic transformation

SFE: Stacking fault energy

DF: Driving force

BCT: Body-centered tetragonal

HCP: Hexagonal close-packed

LIST OF SYMBOLS

SYMBOLS

α': Body centered tetragonal martensite

γ: Austenite iron

ε: Hexagonal closed packed martensite

$\Delta G_{M_S}^{\gamma \rightarrow \alpha'}$: Critical driving force for $\gamma \rightarrow \alpha'$transformation

T_0: Temperature at which α and γ have identical composition and free energies

CHAPTER 1

INTRODUCTION

Austenitic manganese steel, also commonly known as "Hadfield manganese steel", is a type of steel with a high manganese content. It takes its name from the British metallurgical engineer Sir Robert Hadfield, because Hadfield developed this steel in 1882. According to the ASTM Standard A128-64, the composition range is 1-4 wt.% C and 10-14 wt.% Mn. In order to dissolve carbides and create homogenous austenite, Hadfield steel is often austenitized. This homogeneous austenite is then preserved by water quenching at temperatures above 1000°C. Due to the superior performance, especially in properties such as impact resistance and wear resistance, it is especially used in industries where wear conditions are intense, such as mining, quarries, crushers and grinders [1]. Therfore, a comprehensive analysis is important to understand material properties such as microstructures, deformation behaviors and strength.

Austenitic manganese steels represent a class of special steels that differ from other types of steel due to their particularly high manganese content. The properties of these steels are heavily affected by the alloying elements. The effects of alloying elements require steel manufacturers and engineers to carefully design steel compositions to meet specific application requirements. For better material properties, alloying elements and their proportions must be carefully selected.

Alloy design is a discipline that involves designing the composition and processing conditions of a particular material in order to optimize its properties or make it suitable for a specific application. Therfore, this process is used to examining the properties of the Hadfield steel to specific requirements. Computational materials engineering is the process of understanding and optimizing material behavior using computer-based simulation, modeling and analysis methods. Traditional experimentation and prototyping methods are time consuming and costly.

Computational materials engineering can greatly speed up these processes and reduce costs. Material properties can be analyzed in detail and lead to a more comprehensive understanding. In this way, it may be possible to optimize the material for a specific application and increase its performance. It can also be used as a tool for the design and discovery of new materials and components. Thus, computational materials engineering methods play an important role in material design and performance optimization.

Due to their areas of use, Hadfield steels are exposed to impact loads and friction and therefore undergo deformation. The phase transformation can occur due to deformation in the metastable austenite phase. SFE is effective in determining the deformation mode in deformation-induced transformations. Martensitic transformation is one of the transformations expected to occur as a result of deformation in these steels.

In this study, the effect of a wide spectrum of alloying elements on the martensitic transformation related properties of austenitic manganese steels are analyzed using computational techniques. Investigated parameters include Martensite Start Temperature (Ms), Deformation Martensite Start Temperature (Md(50/30)), T-zero and Stacking Fault Energy (SFE). A response surface method is used to investigate the individual effects and binary interactions. The data is also used in local sensitivity analysis using multiple linear regression on the complete dataset. Literature lacks such a systematic study conducted on a large dataset. Thus, this study fill the gap in the literature in this aspect.

CHAPTER 2

LITERATURE REVIEW

Fe-Mn based alloys are important class of engineering materials and have attractive mechanical properties in a variety of industrial applications. Hadfield steels, also known as austenitic manganese steels, are subclass of this group (Figure 2.1).

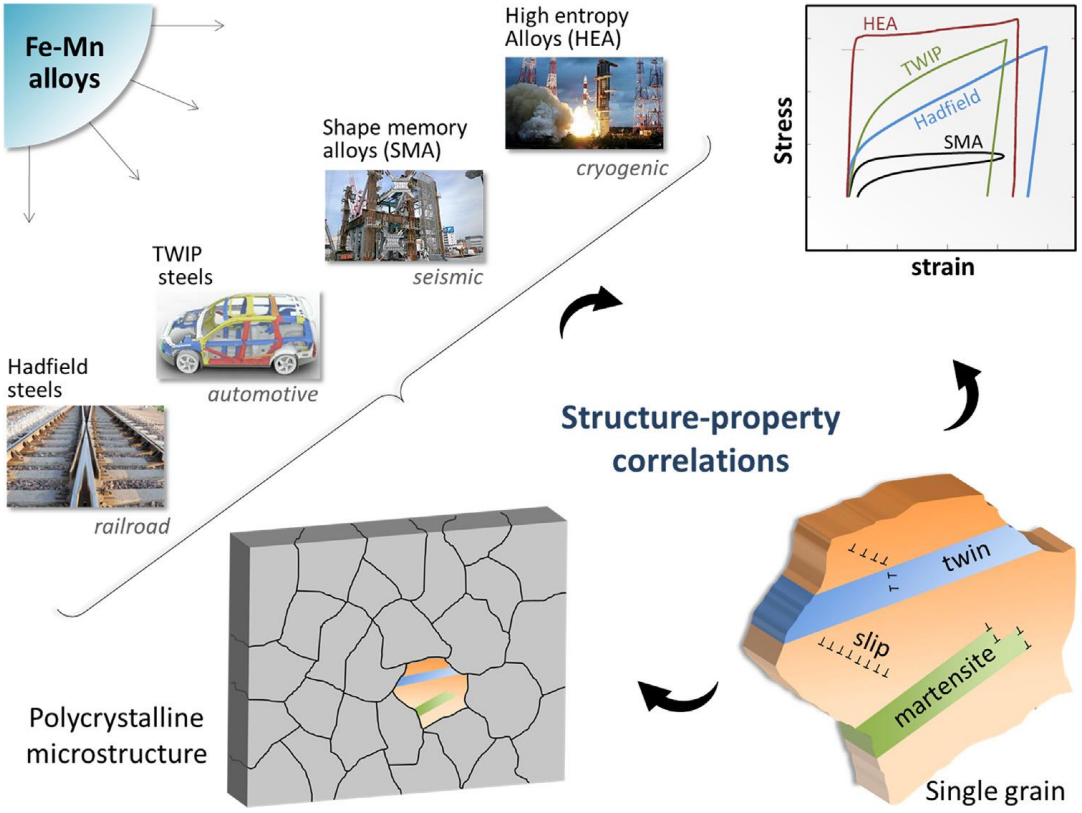

Figure 2.1 Fe-Mn based alloys and their areas of use: railway, seismic, automotive cryogenic applications [2]

2.1 Hadfield Steels

Hadfield steels are used in applications in heavy industry that require wear resistance and high strength. These steels have an outstanding work hardening rate under load and are used particularly in areas such as tracked vehicles, railways, crusher jaws and mining equipment [1,2]. The strength and ductility of Hadfield steel is compared with other structural alloys in Figure 2.2. This excellent steel has good toughness and great work hardening potential. Therfore, it shows high wear resistance together with high strength and ductility [3,4]. Hadfield steels have an austenitic (fcc) structure containing high amounts of manganese. The high strain hardening for which these steels find wide industrial use has been associated with the interaction of dislocation with twinning and interstitial elements such as carbon [3,5,6]. These alloys emerge as interesting case studies because their strengthening properties tend to be enhanced. This is directly related to the fact that the alloy has a low stacking fault energy and this is quite suitable for twinning [3]. In terms of research, important studies have been recorded in the literature on subjects such as deformation mechanisms and alloy effects.

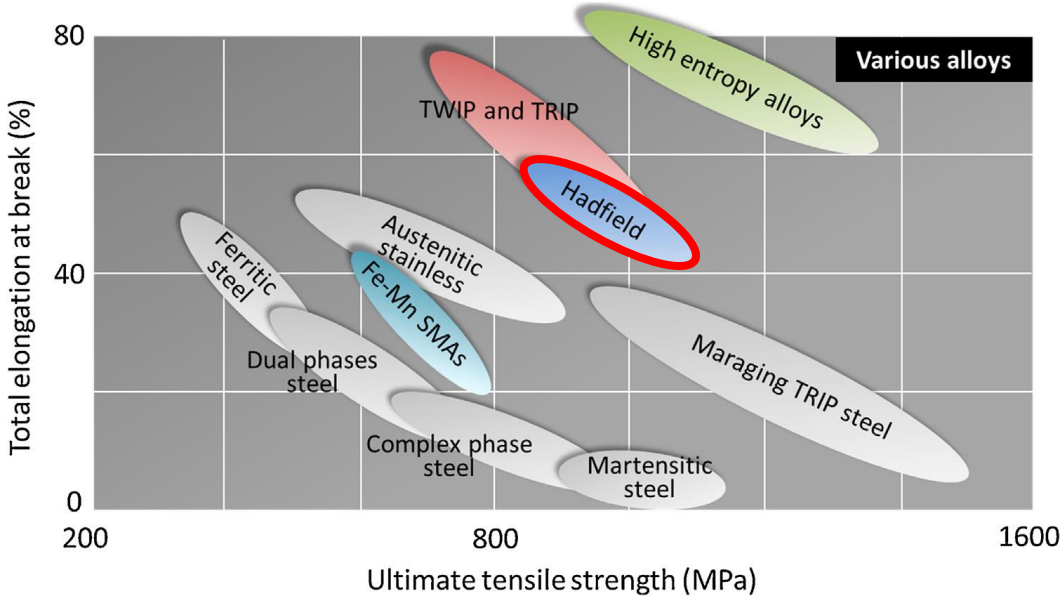

Figure 2.2 Strength and ductility performance exhibited by Hadfield steels among others [2]

Although the composition ranges determined by the ASTM Standard [7] for austenitic manganese steel are 1.0–1.4 wt.% carbon and 10.0–14.0 wt.% manganese, there are many changes in the original chemical composition of austenitic manganese steel. These changes usually involve changes in carbon and manganese and may occur in the presence or absence of additional alloys such as chromium, nickel, molybdenum, and titanium [8].

Hadfield manganese steel castings are generally not useful in the form of as-cast. Because the inevitable carbide formation leads to a loss of ductility and impact toughness. To produce high quality Hadfield steel, austenitizing followed by water quench is generally applied. Complete dissolution of carbides requires solution treatment at 30–50 °C above A_{CM}. The pouring is generally below 1470 °C in order to reduce chemical segregation and avoid coarse grain size [8]. A temperature of around 1010–1120 °C is used for solution heat treatment. To avoid internal cracking, a low heating rate is necessary; to avoid carbide formation, a high quench rate is desirable. Table 2.1 provides an overview of the common mechanical properties [2].

Table 2.1 Typical Mechanical Properties of Hadfield steel (1-1.4 wt.% C, 10-14 wt.% Mn) [2]

0.2% Offset Yield Strength	379 MPa
Ultimate Tensile Strength	965 MPa
Elongation	50%
Reduction of Area	40%
As Quench Hardness	190 HB
Hardness at Fracture	500 HB
Charpy V-Notch Impact at 22°C	169 J
Charpy V-Notch Impact at -196°C	7 J

2.1.1 Alloying Elements

The main alloy component of Hadfield steel, manganese (Mn), is essential for stability of austenite and retaining of it at room temperature. The maximum fraction of available retained austenite rises with increasing Mn concentration [9]. Around 2-3 wt% Mn addition can result in 20% volume increase in retained austenite[10]. Since Mn slowly diffuses within the austenite, it has a tendency to segregation. Similar to Mn, carbon significantly decreases the Ae1 and Ae3 temperatures and stabilizes austenite. Additionally, it has a high effect of solid solution hardening [10].

2.2 Martensitic Transformation

Hadfield steels has metastable austenitic matrix phase. After mechanical loading, it can be transformed into martensite. The relationship between temperature and the chemical free energy of martensite and austenite thermodynamically is shown in Figure 2.3. T_0 is the temperature that the chemical free energy of the martensite equals that of austenite. $\Delta G_{M_S}^{\gamma \rightarrow \alpha'}$ is the critical driving force for transformation. It is equal to the energy barrier for transformation that is given by interfacial energy, frictional energy and elastic strain energy. Frictional work is associated with the interface motion and defect formation in the process of transformation. An extra mechanical work (W) must be supplied in order to obtain $\Delta G_{M_S}^{\gamma \rightarrow \alpha'}$ for a temperature below T_0 [11].

The mechanical work is the factor in the formation of stress induced martensite, which resembles as-quenched martensite that forms below the melting point in terms of nucleation behavior. On the contrary, the formation of new nucleation sites is additionally produced by the previous plastic deformation in strain induced martensite. Olson and Cohen suggested that nucleation of BCT α'-martensite nucleation preferentially occurs at various HCP ε-martensite intersections, stacking faults and twins. In high Mn steels and metastable austenitic stainless steels, such

martensite formation can be observed [12]. ε-martensite is another form of martensite possessing HCP structure. It can be observed in medium Mn steels upon deformation. Since the SFE of the austenite in these steels is generally sufficiently low i.e., several tens of mJ m^{-2}, ε-martensite formation can also be expected in Hadfield steels [10,13]. A few volume percent are usually claimed to be the quantity of ε-martensite caused by deformation, which is significantly less than that of α′-martensite. Furthermore, there are studies that ε-martensite exhibits intermediate behavior when deformed at room temperature. Eventually, at higher deformations, it transforms to α'-martensite. Therefore, it can be say that ε-martensite formation due to deformation contributes less to strain hardening when compared to α′-martensite [13–15].

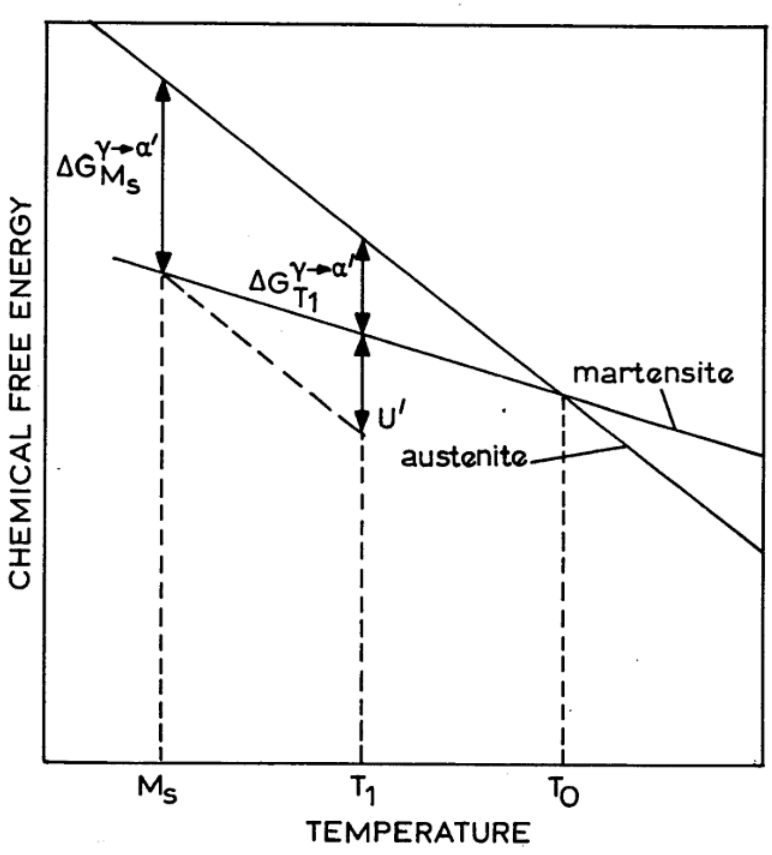

Figure 2.3 The relationship between temperature and the chemical free energy of martensite and austenite [16]

2.2.1 Martensitic Transformation Temperatures

Considering the usage areas of Hadfield steel, the formation of martensite is preferred to occur as a result of athermal processes such as plastic deformation rather than cooling, mostly rapid cooling. Since martensite formed by rapid cooling causes the material to lose its toughness, the material can fail prematurely during use. On the other hand, when martensite does not form after rapid cooling and the material has nearly fully austenite phase, it gains high toughness. When the surface is impacted during usage, martensitic transformation can occur due to deformation on the surface and the material gains wear resistance. At the same time, it preserves its toughness by keeping the inner part in an austenite structure. For this reason, it is desired that only austenite in the surface of the material transforms into martensite. As a result, the material must be above Ms temperature after austenitization followed by cooling. The chemical composition of the alloy significantly affects Ms temperature. It is possible to decrease the Ms by adding certain alloying elements. For example, 1 wt.% Mn addition can cause to lower the Ms temperature by 30-40°C [9].

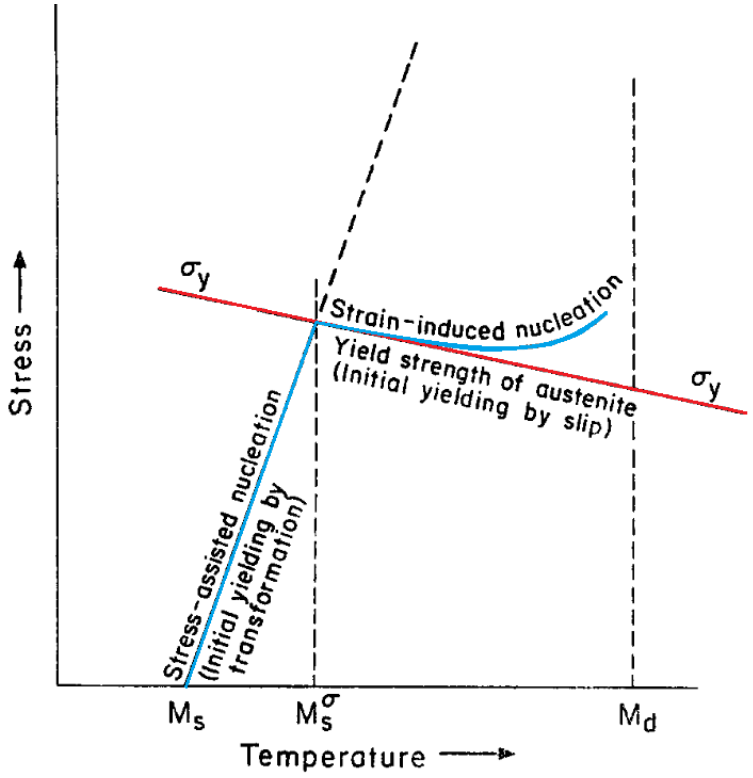

Figure 2.4 Stress-assisted and strain-induced nucleation of α' martensite in Fe-Ni-C alloys. [12]

Figure 2.4 indicates the critical martensitic transformation temperatures for stress-assisted and strain-induced nucleation of α' martensite in Fe-Ni-C alloys. The necessary initiating stress is below σ_y (in the elastic range). Since chemical driving force decreases, required stress for transformation increases. Between M_s^σ and *Md*, firstly, plastic deformation begins. Then, strain hardening occurs with increasing stress beyond σ_y. Strain-induced nucleation starts with further increase in stress. Md temperature is a limit for the formation of deformation induced martensite, and martensite does not form above this temperature. Therefore, it is desired that the material must be below Md temperature during use. However, since it is very difficult to determine this temperature, another parameter, Md (50/30) temperature, is used. It is the temperature at which 50% of the material turns into martensite when 30% deformation is applied to the material [17]. Therefore, transformation of 50%

of the austenite to martensite can be seen under the strain of 30%. About 10°C reduction in Md is possible by adding 1 wt.% Mn [9,18].

2.3 Stacking Fault Energy

In general, stacking faults are caused by dislocation dissociations. The driving force behind the formation of such defects is the dislocation energy minimization [19].

There are many studies in the literature examining the relationship between deformation mechanism and stacking fault energy. In this way, SFE ranges and the occurrence of different mechanisms are determined. In the estimation, SFE is taken to be the Gibbs energy needed to form an ε martensite platelet with only two atomic layer thickness [20]. Depending on the stacking fault energy, displacive transformations may occure during plasticity according to the data in the literature. Accordingly, it has been noted that ε martensitic transformation takes place for SFE < 18 mJ m^{-2} and mechanical twinning occurs for 12 mJ m^{-2} < SFE < 35 mJ m^{-2}. It can also be accepted that slip takes place for SFE > 45 mJ m^{-2} [21–23].

The chemical composition of the alloy and temperature affect stacking fault energy. The literature includes many studies related to effect of alloying elements on it. Since SFE is effective in determining the deformation mechanism, Hadfield steel's mechanical properties and related deformation mechanisms are significantly affected by the addition of alloying elements. For instance, Zudeima et al. observed that Al suppresses the twinning propensity by raising the stacking fault energy [24].

Since Hadfield steels contains medium-high Mn content, the comprehension of how Mn concentration affects stacking fault energy is important. SFE of the austenite at ambient temperature has been demonstrated for Fe-Mn alloys to first lowering and then rising with increasing Mn concentration. This leads to a parabolic dependence of the SFE of the austenite on the Mn content [9,25]. The lower part of the parabolic curve which is the minimum SFE corresponds to Mn concentration between 10-16 wt.% [26]. Mn content in Hadfield steel is between these ranges.

Higher C content raises the austenite's SFE. For every 0.1 weight percent C, SFE increases roughly 2.5- 4 mJ m^{-2}. This has an important effect on the austenite's strain-hardening capacity and deformation behavior [27,28].

Researches indicates that an addition of 1 weight percent Al in solid solution causes the austenite's SFE to rise by about 8.5 mJ m^{-2}. This shows that Al suppreses the ε-martensite formation caused by deformation [29,30].

According to the experimental results, Si has a lowering influence on SFE of austenite i.e., 2-3.5 mJ m^{-2} per weight percent Si. On the other hand, Dumay et al. [31], predict that Si first causes increase in the SFE at low concentrations, then decreases it at greater ones.

2.4 Computational Materials Engineering

Computational materials engineering is the field of materials science and engineering that uses computational methods such as modeling and data analysis. These methods can be used for predicting their properties and understanding material behavior. Computational materials engineering involves the integration of mathematical and computational techniques to analyze material systems. This field focuses on predicting material properties and performance through the use of computer simulations and modeling techniques. In this way, it is possible to design and develop materials faster and more efficiently.

ThermoCalc and JMatPro are computer-based software used to calculate the thermochemical and thermodynamic properties of materials. They can be used to calculate temperatures critical for martensite transformation and stacking fault energy. These software have a large database for modeling material properties.

Through the reduction of high costs, time, and material resources involved with experimental production and processing of materials, computational tools can expedite the design and improve alloy processing. These tools can contribute to the

development of faster, cheaper and more sustainable innovations in materials and components [32].

2.5 Linear Regression

Linear regression method can be used through a set of uncertain data points in order to determine the best straight line. Besides calculating the intercept and slope of this straight line can be discussed. Also, methods for evaluating the validity of the results can be presented.

$$\textit{Simple Linear Regression: } y = a_0 + a_1 x_1$$

$$\textit{Multiple Linear Regression: } y = a_0 + a_1 x_1 + a_2 x_2 \ldots a_n x_n$$

When the dependent variable, *y*, is a linear function of two or more independent variables x_1, x_2, … x_n, *multiple linear regression* is intended to be used. When analyzing experimental data when the variable of interest depends on several different factors, this approach is especially useful. For instance, *y* can be a linear function of x_1 and x_2.

$$y = a_0 + a_1 x_1 + a_2 x_2$$

When fitting the data where the variable in study is frequently a function of two other variables, this equation can be useful. As depicted in Figure 2.5, the regression line appears as a plane for two dimensional case [33].

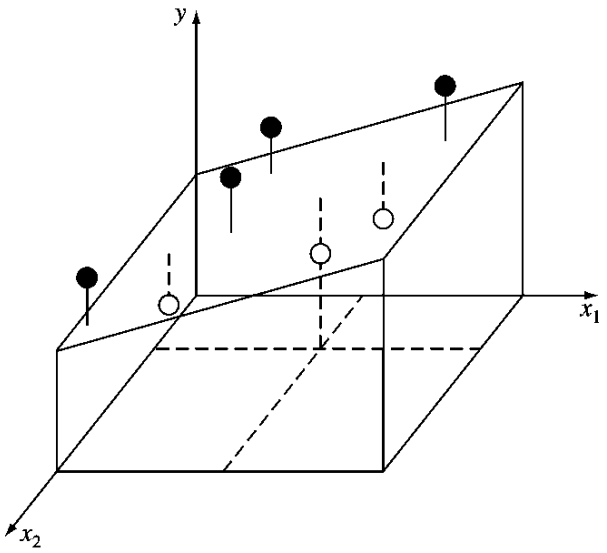

Figure 2.5 Multiple linear regression represented graphically, with y being a linear function of x_1 and x_2 [33].

In regression analysis, there is also an important concept called *interaction terms*. In order to examine that the relationship between the dependent and independent variables is affected by another independent variable, interaction terms are used. It is effectively a multiplication of two independent variables having a joint effect on the dependent variable. The new model can be expressed by the following equation.

$$y = a_0 + a_1 x_1 + a_2 x_2 + a_3 x_1 x_2$$

a_0 is the intercept; a_1, a_2 and a_3 are the other coefficients of the model. a_3 represents the interaction between x_1 and x_2. It specifies the magnitude and direction of the interaction between the relevant independent variables. For instance, a positive interaction coefficient indicates that as the value of one independent variable increases, the effect of the other independent variable also increases. Conversely, a negative interaction coefficient suggests that as the value of one independent variable increases, the effect of the other independent variable decreases. In summary, the interaction term and its coefficients determine the interaction between different variables in a regression model and quantify the magnitude of this interaction. This

interaction term increases the flexibility of the model in cases where the relationship between x_1 and x_2 is non-linear. For example, the effect of x_1 may vary depending on the value of x_2, or the effect of x_2 may vary depending on the value of x_1. [34].

2.6 Sensitivity Analysis

In mathematical model of any process, there can be uncertainties in input data, such as experimental errors. The accuracy of the input data is crucial to getting reliable simulation results. It can be improved by increasing the number of experiments, but these significantly raise the cost and time needed. This is especially true for understanding the effect of alloying elements on properties of Hadfield steels since a vast number of alloys need to be determined through experimentation. These difficulties can be solved by implementing a model and performing sensitivity analysis. Therefore, in general terms, the purposes of sensitivity analysis in various contexts are designing experiments, estimating errors, assessing model accuracy and informing data collection strategies. [35].

It is common to use a sensitivity analysis to look into how the models behave.This involves observing how the dependent variable changes as the independent variables change [33]. Sensitivity analysis can be defined as a local measure of the influence of a certain input on a certain output. It is used to determine how the input and output variables relate to one another. This is achieved by calculating the system derivatives like following equation.

$$S_j = \frac{\partial y}{\partial x_j}$$

where x_j is the input factor and y is the output of interest [36].

In order to perform sensitivity analysis, a model or system must first be created. It should then be exposed to different values of the input variables in this model or system and observed how the output variables change. Sensitivity analysis is performed to understand how these changes affect the outputs. This analysis is

usually performed to determine the effects of various input variables, evaluate the sensitivity of the model, and evaluate the reliability of the results.

The mathematical model for the analysis can be expressed as

$$f_i(x_1, x_2, \ldots, x_j) = y_i$$

x_j is the input parameters (wt.% of alloying elements) and y_i is the output parameters (stacking fault energy, martensitic transformation temperatures).

Once a sufficient number of inputs have been utilized to detect a linear trend within the implemented model, sensitivity parameters are determined using the derivatives of the trendlines. Sensitivity analysis can be enhanced and generate more outputs by examining the results of changing multiple parameters at once. In this case, the partial derivative of the function with respect to input variable x_j is taken by using the mathematical model for the analysis. For example, following equation can be considered.

$$y = a + bx_1 + cx_2 + dx_1x_2$$

In this equation, *interaction terms* expressing the relationship between the dependent and independent variables is affected by another independent variable exist. The coefficient d represents the interaction between x_1 and x_2. Thus, the relationship between the variables x_1 and x_2 can be represented in the model in a non-linear manner.

By using this model, the partial derivative of y with respect to x_1 and x_2 gives sensitivity values, $b + dx_2$ and $c + dx_1$, respectively.

$$\frac{\partial y}{\partial x_1} = b + dx_2 \qquad \frac{\partial y}{\partial x_2} = c + dx_1$$

In this way, two input parameters, x_1 and x_2, are modified at once and their interactions are examined.

CHAPTER 3

MATERIALS AND METHODS

3.1 Metallographic Specimen Preparation

Although this thesis is mainly a computational study, some microstructural investigations are performed on GX120Mn12 to have an insight about the real microstructure of real austenitic Mn-steel. The standard metallography steps are followed for the sample. Firstly, the sample is cut into smaller sizes by precision cutter. Then, the mounting of the samples using bakelite powder mixture is performed. Afterwards, the samples are grinded by using different grades of emery papers as follows; 120-320-600-800-1000-1200 under rotating disc grinder. The samples are polished with 6 μm followed by 1μm diamond solutions under rotating disc polishers after final grinding. Finally, etching of the polished specimen is performed for 10-15 seconds with Nital's reagent at concentration of 2%. Specimens are examined under HUVITZ optical microscope. Micrographs are taken under different magnifications.

3.2 The Effect of Alloying

In this study, the CALPHAD approach, which offers thermodynamic modeling of multi-component materials, is employed for thermodynamic-based modeling. Calculations are done by using JMatPro v14.0 and Thermo-Calc version 2021a. The TCFE11 database is used in Thermo-Calc for the prediction of the material properties thermodynamically. The effects of Al, Mn, Cr, Mo, Cu, Nb, Co, Ni, O, V, Si, B alloying elements on properties are predicted by using computational tools depending on each alloying element and its weight percentages.

Table 3.1 Alloying elements and their weight percentages used in calculation of material properties

Al	Mn	Cr	Mo	Cu	Nb	Co	Ni	O	V	Si	B
0	5	0	0	0	0	0	0	0	0	0	0
0.2	7	1.5	0.2	0.2	0.2	2	2	0.002	0.1	0.2	0.01
0.4	9	3	0.4	0.4	0.4	4	4	0.004	0.2	0.4	0.02
0.6	11	4.5	0.6	0.6	0.6	6	6	0.006	0.3	0.6	0.03
0.8	13	6	0.8	0.8	0.8	8	8	0.008	0.4	0.8	0.04
1	15	7.5	1	1	1	10	10	0.01	0.5	1	0.05
-	17	9	1.2	-	-	-	-	-	-	1.2	-
-	19	10.5	1.4	-	-	-	-	-	-	1.4	-
-	21	12	1.6	-	-	-	-	-	-	1.6	-
-	23	13.5	1.8	-	-	-	-	-	-	1.8	-
-	25	15	2	-	-	-	-	-	-	2	-

The different amount of each alloying element given in Table 3.1 are added one-by-one to the standard composition of GX-120Mn12 steel. In this way, single element variations are analyzed and calculated property data is generated. In this regard, stacking fault energy (SFE), martensitic transformation temperatures (Ms and Md(50/30)) are calculated by using JMatPro. T-Zero temperature and Ms temperature (to compare with JMatPro results) are calculated by using Thermo-Calc. Graphs are created using the calculation results. Chemical composition of standard GX-120Mn12 Hadfield steel using in calculations is given in Table 3.2.

Table 3.2 Chemical composition of EN/DIN GX-120Mn12 Hadfield steel

Element	Fe	Cr	Cu	Mn	Si	C	P	S
Wt.%	83.96	1.5	0.3	12.5	0.4	1.2	0.1	0.04

CHAPTER 4

RESULTS AND DISCUSSION

Within the scope of the thesis, this chapter contains the results of microstructures studied under optical microscope and the calculations carried out with the computational tools. Process parameters are predicted with the help of thermodynamic and kinetic calculations.

4.1 Microstructural Analysis

The specimens are studied under the optical microscope to obtain information about the microstructure. This part gives information about the grains and grain boundaries. GX120Mn12 steel specimen is produced by casting in Pınar Döküm®, İzmir/Türkiye. Heat treatment is applied at 1100°C and cooled. Figure 4.1 shows the microstructures of GX120Mn12 steel obtained by using optical microscopy. Austenite grains and grain boundaries can be seen in the figures arranged according to different magnifications. As-cast material has austenitic matrix and large carbides along grain boundaries. Since homogenization heat treatment is applied to this specimen, microstructure contains mainly FCC matrix with small and low amount primary carbides.

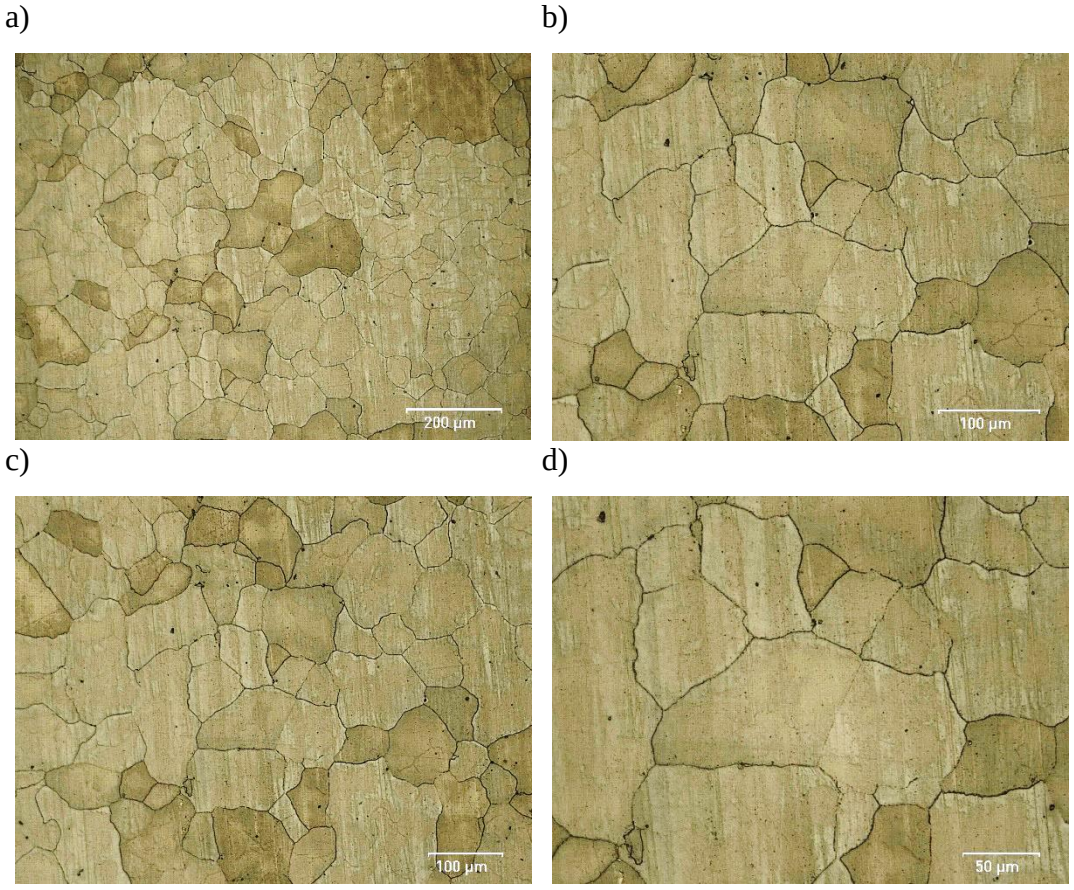

Figure 4.1. Microstructures of GX120Mn12 steel applied heat treatment at 1100°C under different magnifications obtained by optical microscopy.

4.2 Stacking Fault Energy (SFE)

Stacking faults have an initiating effect on martensite transformation. The one mentioned here is ε-martensite with hexagonal close-packed (HCP) structure. Martensite nucleation may occur due to stacking faults. If the stacking energy (SFE) is low, the tendency to turn into martensite through deformation is greater. Therefore, SFE can determine the formation of martensite. It is known that manganese in Hadfield steel affects martensite transformation by reducing SFE in certain compositions (Figure 4.2, B). At the same time, this low energy also encourages the formation of deformation twins in austenite grains. Thus, it positively affects the

strength by increasing the interaction with dislocation. It is also thought that martensite nucleation may occur where twinning occurs. This nucleation also has the effect of initiating the martensite transformation. Although it varies from study to study, an SFE value of 20 mJ/m2 can be recommended as an upper limit for the formation of deformation induced martensite [29]. Accordingly, at values lower than 20 mJ/m2, the metastable austenite phase turns into ε-martensite (HCP). The SFE value for the formation of deformation twins varies between 12 mJ/m2 and 35 mJ/m2 [37]. Therefore, alloying elements that reduce SFE are preferred for martensite transformation.

In this study, SFE values are calculated using JMatPro. In Figure 4.2, SFE values varying depending on the weight percentages of alloying elements were examined at room temperature and 200°C. Here we see the chromium, which behaves differently compared to other elements (Figure 4.2,C). Chromium has an effect of increasing SFE up to 6% and decreasing SFE after 6%.

On the other hand, since the alloying elements are not added to the material in the same amount, sensitivity graphs are created by taking the slopes of the lines in the graphs into account in order to see their effects better (Figure 4.5). In this graph, only the range with an increasing effect is shown for chromium. Considering other elements, aluminum and silicon significantly increase SFE; It is seen that boron, niobium and oxygen are the elements that significantly reduce SFE (Figure 4.5, SFE).

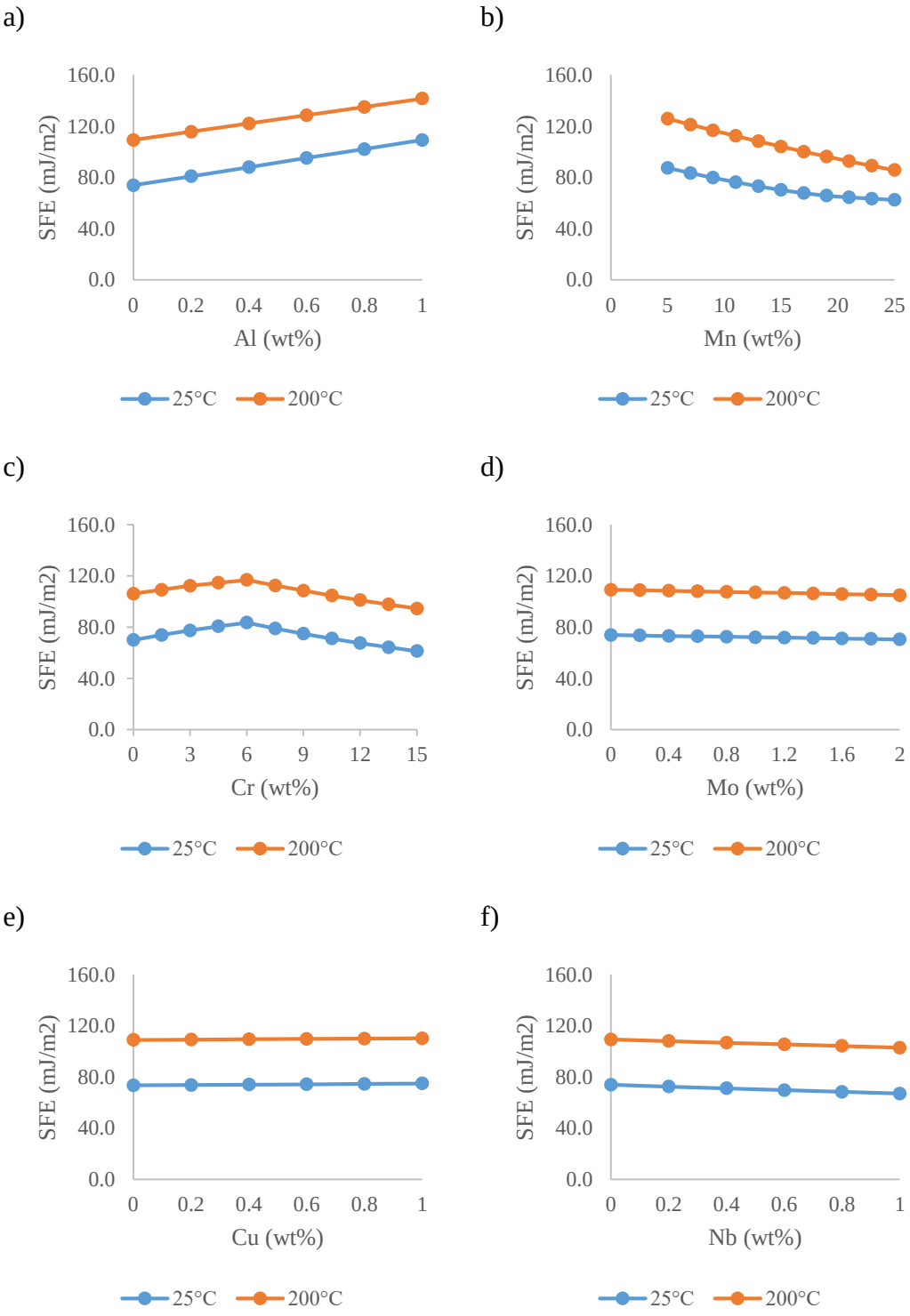

Figure 4.2 Stacking fault energy (SFE) at 25°C and 200°C, varying depending on the weight percentages of the alloying elements

g)

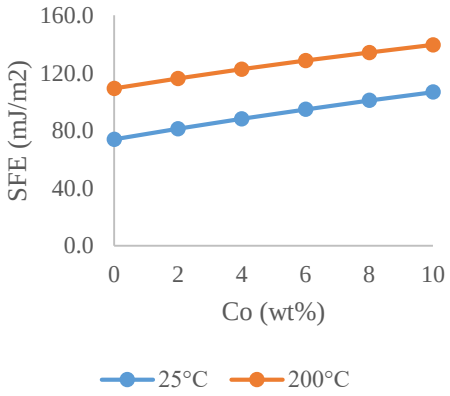

h)

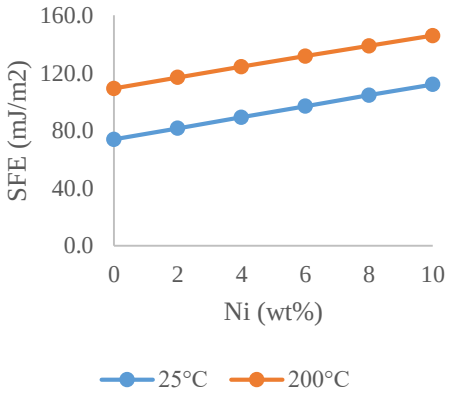

i)

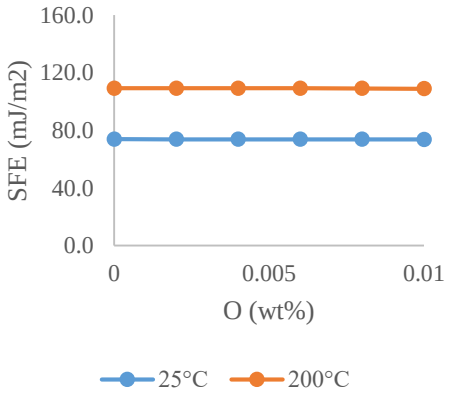

j)

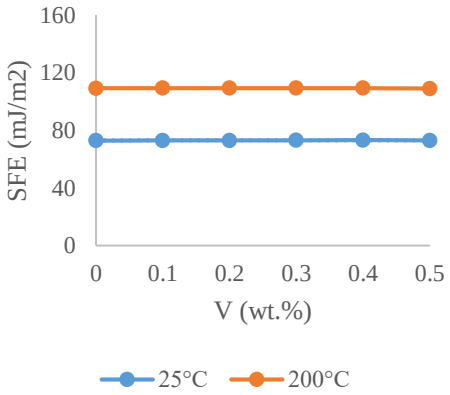

k)

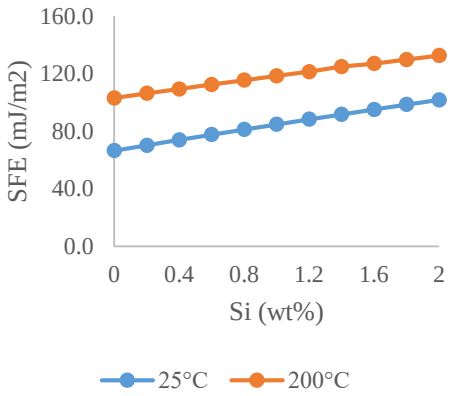

l)

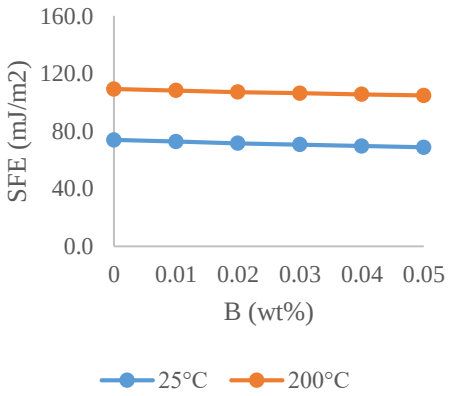

Figure 4.2 (Cont'd)

m)

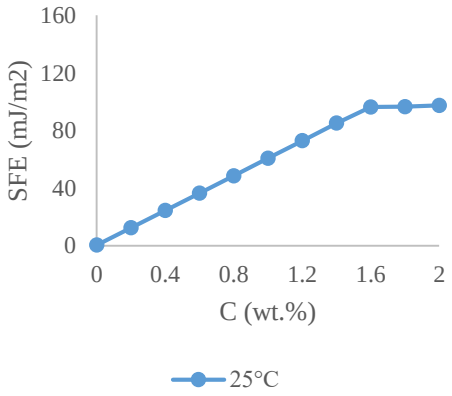

Figure 4.2 (Cont'd)

4.3 Martensitic Transformation Temperatures

4.3.1 Ms

When the results obtained from JMatPro and Thermo-Calc software are examined, although it varies depending on the composition, the martensite initial temperature (Ms) cannot generally be determined in Hadfield steel. This means that for most compositions examined, martensite will not form thermally even when cooled to -273°C. According to JMatPro calculations, when high amounts of cobalt or low amounts of manganese are used, the Ms temperature does not rise above approximately -140°C (Figure 4.3;D,E). According to Thermo-Calc results, the highest Ms temperature is -45°C when 5wt.% manganese is used. Generally, these temperatures are well below the temperatures in practical application. Therefore, it can be said that there is no possibility of achieving to these temperatures. Considering that this amount of manganese is not used in standard Hadfield steel, it can be said that the Ms temperature is low enough. The use of high amounts of manganese has a great effect on why the MS temperature is so low.

4.3.2 M_d

It is mentioned that martensite does not form in Hadfield steel during cooling. However, impact and abrasion during use cause microstructural modifications on the surface and martensitic transformation may occur due to deformation. So, even at above Ms, this transformation takes place. Austenite, which is metastable at room temperature, turns into ε-martensite in the HCP structure with deformation. It gains wear resistance under impact. As it is impacted, the material turns into martensite and hardens.

Md(50/30) temperatures are calculated using JMatPro. When the graphs in Figure 4.3 are examined; it is seen that Al, Cr, Mn and Ni elements have a significant reducing effect on Md temperature (Figure 4.3; A,C,E,K). Considering that practical applications are made at room temperature, mass percentages of these elements that reduce the Md(50/30) temperature to -60 degrees should not be preferred. Unlike other elements, Co element has a significant increasing effect on Md temperature (Figure 4.3,D). Considering the sensitivity graph of Md temperature (Figure 4.5, Md(50/30)), it can be seen that the lowering effect of the Al element is higher than the others.

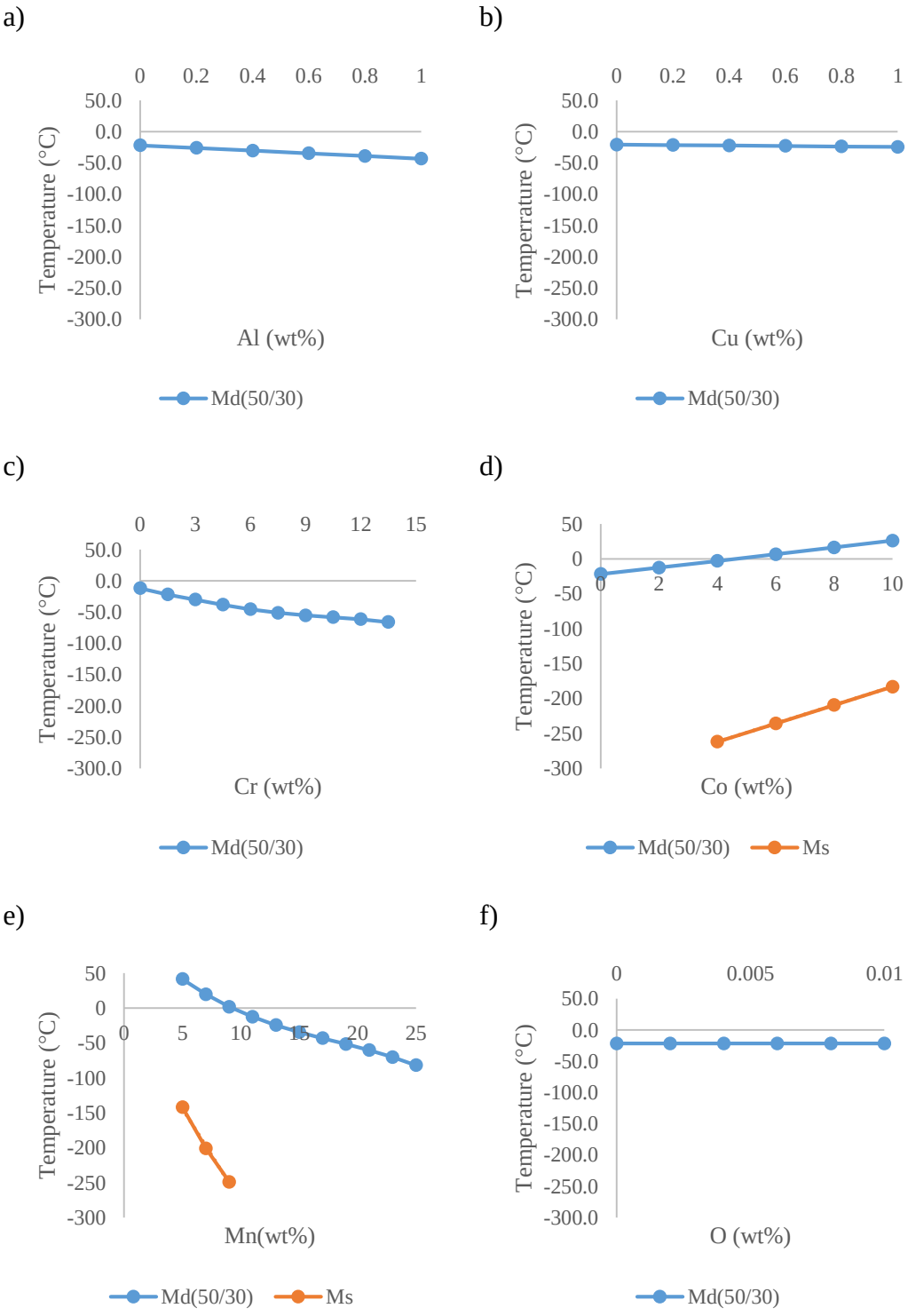

Figure 4.3 Md and Ms temperatures varying depending on the weight percentages of the alloying elements (* Since Ms temperatures is not found for some alloys, they are not given in the graphs)

g)

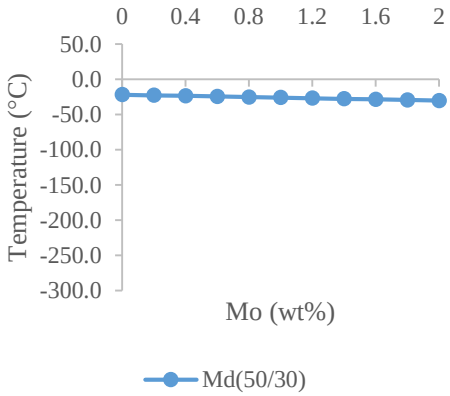

h)

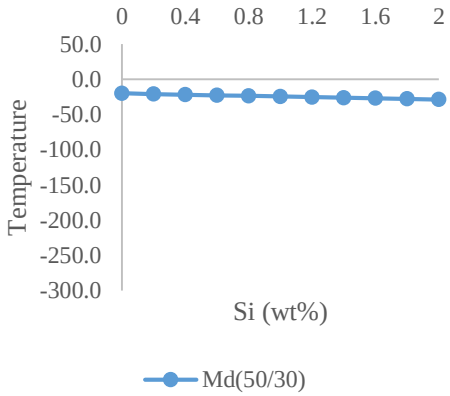

i)

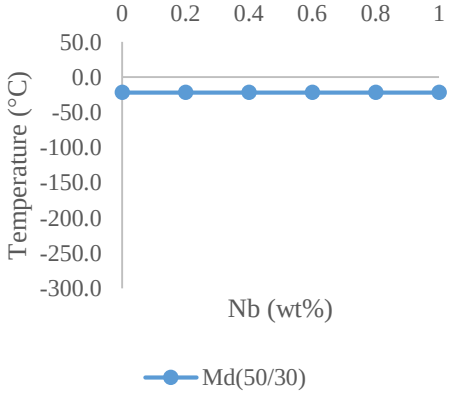

j)

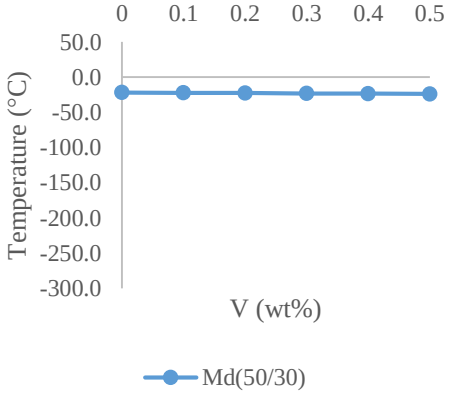

k)

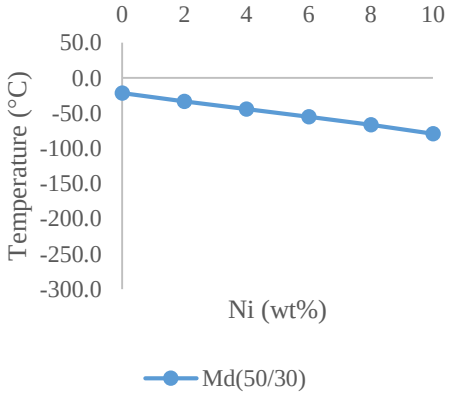

l)

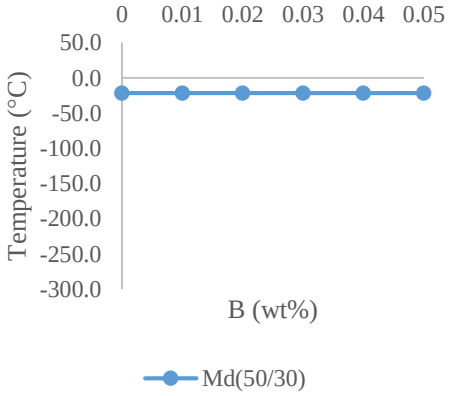

Figure 4.3 (Cont'd)

4.4 T-Zero Temperature

T-Zero temperature is the highest temperature at which the material can undergo athermal phase transformation. Below this temperature, martensitic transformation can occur. At temperatures above T-zero temperature, phase transformations occur by diffusion. In general, elements that decrease the T-Zero temperature also decrease the Ms and Md temperatures. In this study, T-Zero temperatures are calculated using Thermo-Calc. When the graphs are examined, it is seen that Cr and Co elements significantly increase the T-Zero temperature (Figure 4.4;C,D), while Mn element decreases it (Figure 4.4,E). Sensitivity graphs of alloying elements show the significant effect of boron and oxygen on T-Zero temperature (Figure 4.5, T-Zero). Even when added in relatively small amounts, boron element causes this temperature to decrease and oxygen causes it to increase. In the B, E, I, K and L graphs in Figure 4.4, some temperature values corresponding to weight percentages are not shown. Because Thermo-Calc shows T-Zero temperatures here at 1700 degrees. Since there cannot be a T-Zero temperature above the melting point, there are probably errors in the calculations here.

Considering that the martensitic transformation will occur below T-Zero temperature, this temperature can be expected to give results related to Ms and Md temperatures. In general, it was mentioned that elements that lower the T-Zero temperature can also reduce the Ms and Md temperatures. However, when the C and G graphs in Figure 4.3 and the C and G graphs in Figure 4.4 are examined together, it is seen that Cr and Mo elements increase the T-Zero temperature and decrease the Md temperature. At the same time, boron, oxygen and niobium do not affect the Md temperature; Boron and niobium decreased the T-Zero temperature, while oxygen caused a slight increase in the T-Zero temperature (Figure 4.3;F,I,L and Figure 4.4;F,I,L). These results may be due to calculation differences between JMatPro and Thermo-Calc software. Other elements affected T-Zero and Md temperatures as expected.

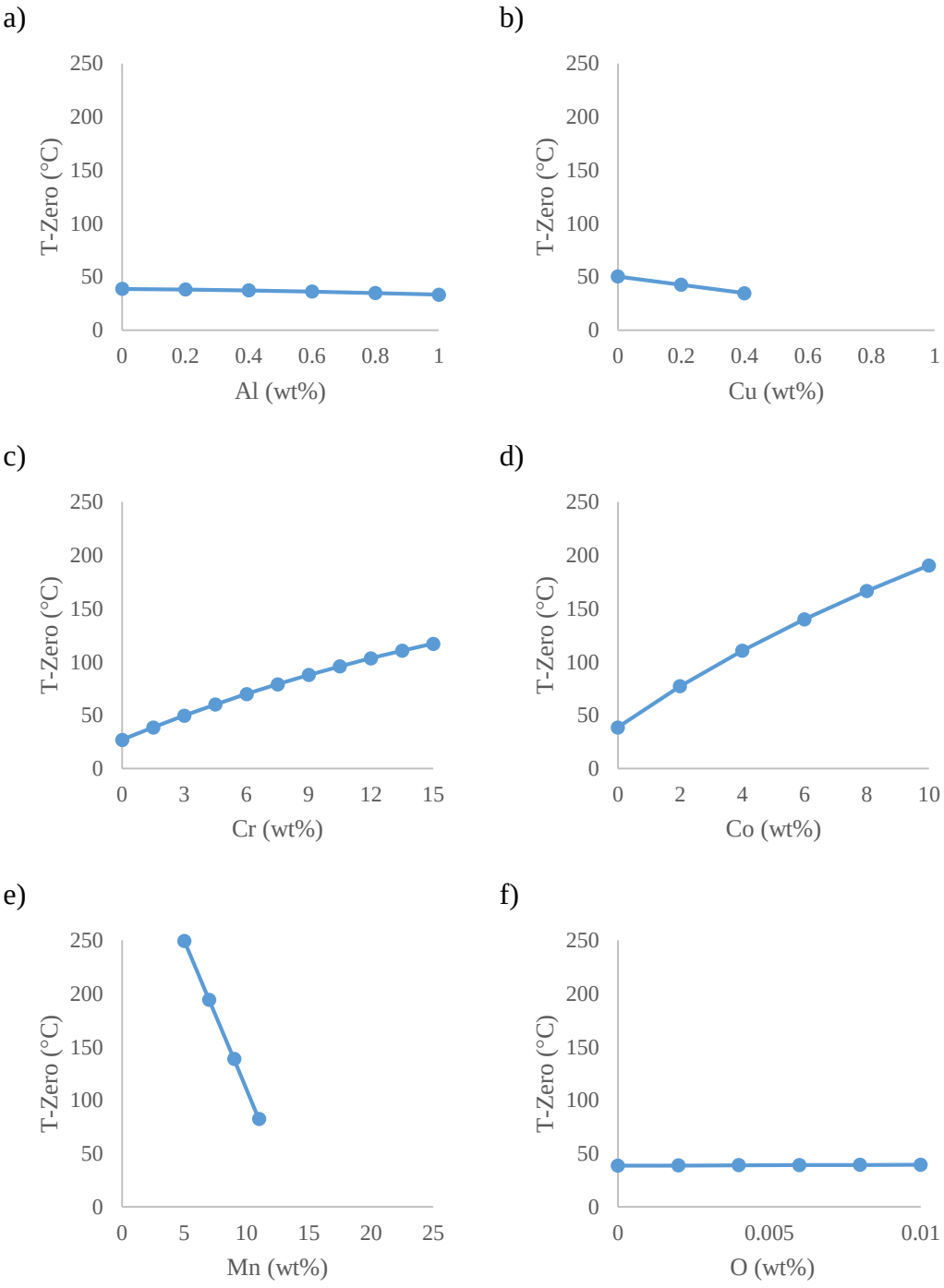

Figure 4.4 T-Zero temperatures vary depending on the weight percentages of the alloying elements (*Since T-Zero is not found for Ni, it is not given in the figure. Also, some T-Zero values are missing for Cu, Mn, Nb and B)

g)

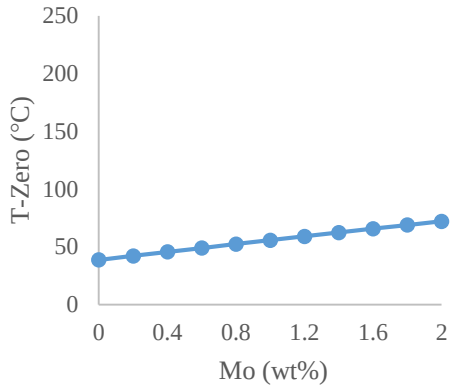

h)

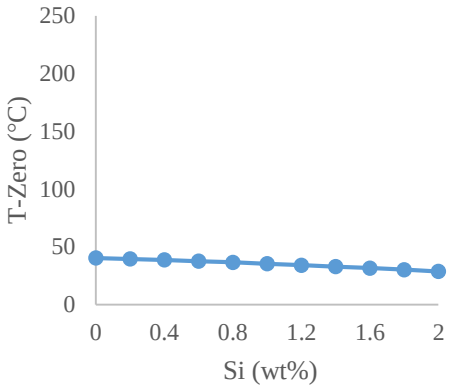

i)

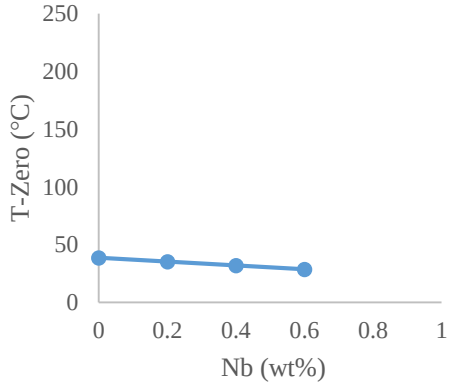

j)

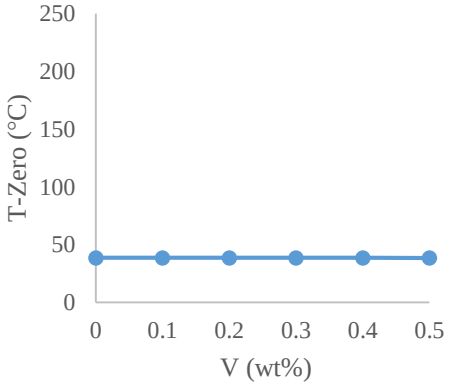

k)

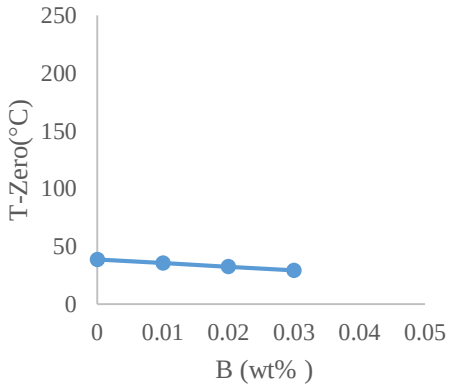

Figure 4.4 (Cont'd)

4.5 Sensitivity Analysis

Sensitivity graphs are plotted to better understand and interpret the effects of unit change in chemical composition on SFE, Md temperature and T-Zero temperature (Figure 4.5). For this purpose, the slopes of the lines in the previous graphs (Figures 4.2, 4.3, 4.4) are calculated and the relative effect of each element on each parameter examined is obtained (Figure 4.5). The higher the slope, the greater the effect of the element; the negative value of the slope indicates that it has a negative effect on the characteristics examined. In this way, the evaluation of the results is simplified by classifying the parameters.

a)

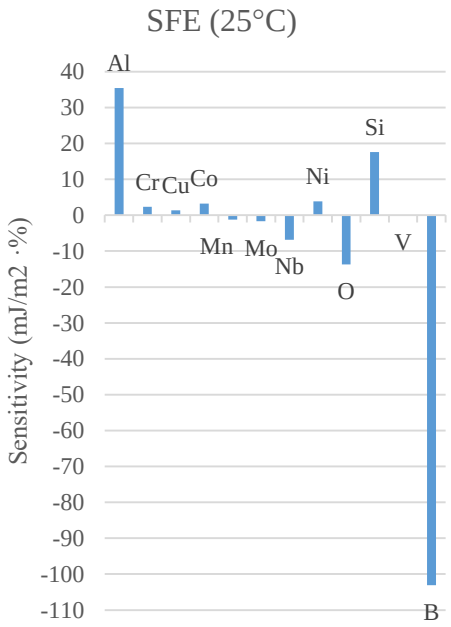

b)

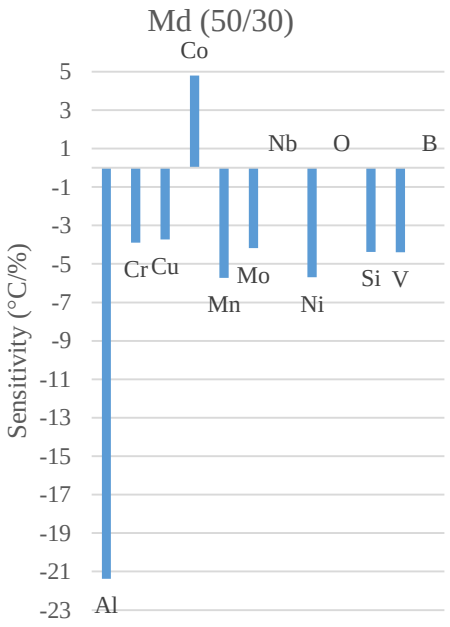

c)

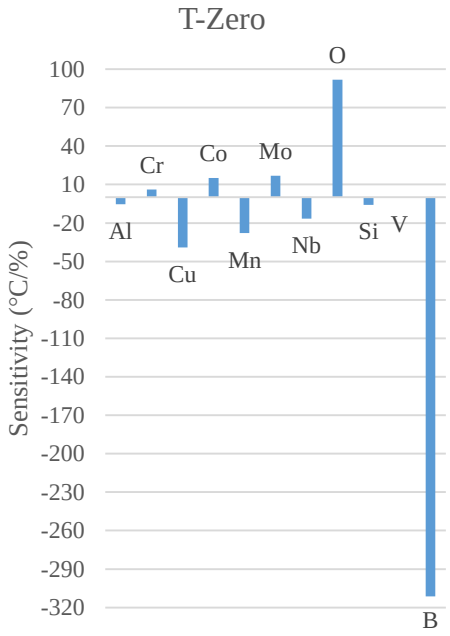

Figure 4.5 Relative effects of alloying elements on SFE, Md temperature and T-Zero temperature.

In the analysis above, only the effect of one alloying element on the properties is studied. This can be called the effect of a single variable. On the other hand, in order to study the effect of two or more alloying elements together on the properties, the interaction between the independent variables (e.g., Mn and Cr) need to be examined. In this case, interaction analysis can be performed to evaluate the interaction between two alloying elements (e.g., Mn and Cr). This is especially useful to understand how two or more independent variables interact together.

Within the scope of this thesis, interaction analysis is performed in order to understand the effect of alloying elements on *stacking fault energy* in GX120Mn12 steel. Weight percentages of alloying elements are used as independent variables and SFE is used as dependent variable. In this study, there are 13 alloying elements to examine:

Cr	Mn	Mo	Si	Al	Cu	Co	Nb	Ni	O	V	B	C

$$C(13,2) = \binom{13}{2} = 78$$

The process of selecting 2 alloying elements out of 13 creates 78 different combinations. These are shown in Table 4.1.

Table 4.1. 2-combinations of 13 alloying elements indicated by "X".

	Cr	**Mn**	**Mo**	**Si**	**Al**	**Cu**	**Co**	**Nb**	**Ni**	**O**	**V**	**B**	**C**
Cr		X	X	X	X	X	X	X	X	X	X	X	X
Mn			X	X	X	X	X	X	X	X	X	X	X
Mo				X	X	X	X	X	X	X	X	X	X
Si					X	X	X	X	X	X	X	X	X
Al						X	X	X	X	X	X	X	X
Cu							X	X	X	X	X	X	X
Co								X	X	X	X	X	X
Nb									X	X	X	X	X
Ni										X	X	X	X
O											X	X	X
V												X	X
B													X
C													

After determining the 2-combinations of alloying elements, change in *stacking fault energy* caused by the unit change in the wt.% of an alloying element with interaction of other alloying elements is examined according to the wt.% of alloying elements given in the Table 4.2.

Table 4.2. The weight percentages of each alloying element used in calculations

Element	**wt.%**										
Cr	0	1.5	3	4.5	6	7.5	9	10.5	12	13.5	15
Mn	5	7	9	11	13	15	17	19	21	23	25
Mo	0	0.2	0.4	0.6	0.8	1	1.2	1.4	1.6	1.8	2
Si	0	0.2	0.4	0.6	0.8	1	1.2	1.4	1.6	1.8	2
Al	0	0.1	0.2	0.3	0.4	0.5	0.6	0.7	0.8	0.9	1
Cu	0	0.1	0.2	0.3	0.4	0.5	0.6	0.7	0.8	0.9	1
Co	0	1	2	3	4	5	6	7	8	9	10
Nb	0	0.1	0.2	0.3	0.4	0.5	0.6	0.7	0.8	0.9	1
Ni	0	1	2	3	4	5	6	7	8	9	10
O	0	0.001	0.002	0.003	0.004	0.005	0.006	0.007	0.008	0.009	0.01
V	0	0.05	0.1	0.15	0.2	0.25	0.3	0.35	0.4	0.45	0.5
B	0	0.005	0.01	0.015	0.02	0.025	0.03	0.035	0.04	0.045	0.05
C	0	0.2	0.4	0.6	0.8	1	1.2	1.4	1.6	1.8	2

Table 4.3 shows the table template used to examine the interaction between two independent variables. There are 11 different wt.% for each alloying elements as giving in Table 4.2. The region where the SFE values are located is 11x11 matrix. An example table with SFE values for Mo and Co elements is shown in Table 4.4. Based on the standard Hadfield steel GX120Mn12 given in Table 3.2, wt.% of two of alloying elements are changed according to the Table 4.2 and wt.% of other alloying elements are taken as constant. Stacking fault energy values are calculated by using JMatPro. An example table with SFE values for Mo and Co elements is shown in Table 4.4. As can be seen here, 121 SFE values are calculated in total just for interaction of Mo and Co. Similarly, calculations are performed for other 78 different combinations. This means that 78 x 121 = 9438 calculations are done in

order to understand the effect of alloying elements on SFE by examining the interaction effect between two independent variables i.e., weight percentages of two different alloying elements. It can be say that independent variables are input parameters and dependent variable is output parameter.

Input parameters: wt.% Cr, wt.% Mn, wt.% Mo, wt.% Si, wt.% Al, wt.% Cu, wt.% Co, wt.% Nb, wt.% Ni, wt.% O, wt.% V, wt.% B, wt.% C

Output parameter: Stacking fault energy

For example, wt.% Mo and wt.% Co as independent variables may display a relationship in the way they affect the SFE as dependent variable. For instance, increasing wt.% of Mo may decrease SFE, but this may also depend on wt.% of Co. The presence of Co can eliminate the decreasing effect of Mo. Therefore, there may be an interaction effect between independent variables besides main effect individually.

Table 4.3. Table template for interaction between two independent variables

	The weight percentages of alloying element A **(1x11)**
The weight percentages of alloying element B **(11x1)**	Stacking fault energy values (mJ/m^2) **(11x11)**

Table 4.4. An example table with SFE values for Mo and Co elements

	0	**0.2**	**0.4**	**0.6**	**0.8**	**1**	**1.2**	**1.4**	**1.6**	**1.8**	**2**
0	72.9	72.5	72.2	71.9	71.5	71.2	70.9	70.5	70.2	69.9	68.7
1	76.6	76.3	75.9	75.6	75.2	74.9	74.6	74.2	73.9	73.5	71.5
2	80.2	79.9	79.5	79.2	78.8	78.5	78.1	77.8	77.5	76.1	74.2
3	83.7	83.4	83	82.7	82.3	82	81.6	81.3	80.7	78.8	76.9
4	87.2	86.8	86.5	86.1	85.8	85.4	85	84.7	83.2	81.3	79.5
5	90.5	90.1	89.8	89.4	89.1	88.7	88.4	87.6	85.6	83.7	82
6	93.7	93.4	93	92.7	92.3	91.9	91.6	89.9	87.9	86.1	84.4
7	96.9	96.5	96.2	95.8	95.4	95	94	92.1	90.2	88.5	86.8
8	99.9	99.6	99.2	98.8	98.4	98.1	96.1	94.2	92.4	90.7	89.1
9	102.9	102.5	102.1	101.7	101.4	100.1	98.1	96.3	94.5	92.9	91.3
10	105.7	105.4	105	104.6	104	101.9	100.1	98.3	96.6	95	93.5

The weight percentages of alloying element A and B are taken as *x* and *y* values, respectively. SFE values, on the other hand, are 11x11 matrix. 3D graph of this table is obtained by defining *x, y* and *matrix* values in MATLAB as shown in Figure 4.6. The matrix contains the *z* values of the values in the x and y coordinates. A compatible plane is fitted using the fit function. It adapts using linear interpolation. A linear regression model is created and the coefficients of the model (a, b and c) are calculated. Using these coefficients, the *plane equation* is obtained. Therefore, *linear regression model* used in analysis is a plane equation:

$$z = a + bx + cy \qquad \text{or} \qquad y = a + bx_1 + cx_2$$

In order to see how output parameter (i.e., SFE) changes as input parameters (i.e., wt.% of alloying elements) are varied, *sensitivity analysis* is performed by using the following equation.

$$S_j = \frac{\partial y}{\partial x_j}$$

According to the linear regression model in this study, the partial derivative of *y* with respect to x_1 and x_2 gives sensitivity values, *b* and *c*, respectively.

$$\frac{\partial y}{\partial x_1} = b \qquad\qquad \frac{\partial y}{\partial x_2} = c$$

In this way, two input parameters (x_1 and x_2 representing the wt.% of alloy A and B, respectively) are modified at once and their interactions are examined. Since there are 11 different wt.% for each alloy, interaction of 2 different alloying elements gives 121 number of observation.

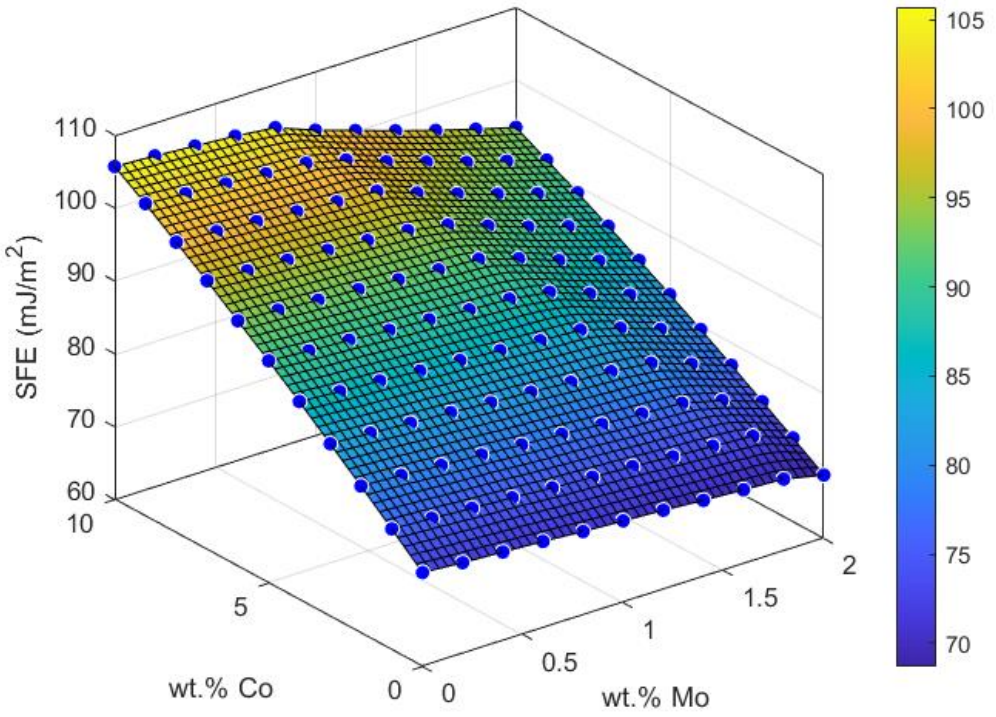

Figure 4.6. An example stacking fault energy calculation results at 25°C, varying depending on the specified weight percent ranges of Co and Mo.

According to the regression analysis; *a, b, c* are estimated coefficients and express the effect of independent variables quantitatively. *a* is the constant term of the linear regression equation, that is, y value when the independent variables are zero. Therefore, *a* is the constant term, that is, the value at the point where the regression

plane intersects the y-axis. This is the expected value of the dependent variable when the value of the independent variables is zero. Table 4.5 shows intercept values for all interactions. Diagonal part of the table is obtained using simple linear regression model ($y = a + bx$). Off-diagonal part of the table, on the other hand, is obtained using multiple linear regression model ($y = a + bx_1 + cx_2$).

Table 4.5. Intercept values for all interactions: Diagonal part is obtained using simple linear regression model and off-diagonal part is obtained using multiple linear regression model.

	Cr	**Mn**	**Mo**	**Si**	**Al**	**Cu**	**Co**	**Nb**	**Ni**	**O**	**V**	**B**	**C**
Cr	79.37	86.40	78.18	82.97	80.84	79.54	84.46	76.76	84.95	78.45	79.51	76.04	23.80
Mn	86.40	91.07	92.18	83.93	90.22	89.48	96.57	87.26	100.5	89.63	89.39	91.05	22.79
Mo	78.18	92.18	73.85	69,62	72.68	72.75	76.16	72.94	77.47	73.00	73.34	72.91	9.43
Si	82.97	83.93	69,62	66.75	66.27	65.44	67.35	66.46	69.65	65.78	66.45	67.02	-4.88
Al	80.84	90.22	72.68	66.27	73.84	72.32	73.59	73.37	73.80	72.88	73.06	72.31	-8.63
Cu	79.54	89.48	72.75	65.44	72.32	73.39	73.35	72.49	72.87	72.49	72.59	72.42	4.80
Co	84.46	96.57	76.16	67.35	73.59	73.35	74.48	73.37	79.72	73.60	74.31	73.90	11.59
Nb	76.76	87.26	72.94	66.46	73.37	72.49	73.37	73.80	72.97	72.87	73.85	72.27	2.11
Ni	84.95	100.5	77.47	69.65	73.80	72.87	79.72	72.97	73.89	73.33	73.76	74.84	9.59
O	78.45	89.63	73.00	65.78	72.88	72.49	73.60	72.87	73.33	73.83	72.92	72.61	4.70
V	79.51	89.39	73.34	66.45	73.06	72.59	74.31	73.85	73.76	72.92	72.95	72.71	4.95
B	76.04	91.05	72.91	67.02	72.31	72.42	73.90	72.27	74.84	72.61	72.71	73.76	8.11
C	23.80	22.79	9.43	-4.88	-8.63	4.80	11.59	2.11	9.59	4.70	4.95	8.11	4.69

In the model, *b* and *c* are the coefficients of the independent variables x_1 and x_2, respectively. They indicate how much the dependent variable will change with the unit change of the relevant independent variables. That is, *b* coefficient expresses how much the *y* variable will change with unit increase in the x_1 variable, and *c* coefficient expresses how much the *y* variable will change with unit increase in x_2 variable. Since the effect of one independent variable may vary depending on the values of other independent variables, binary interaction of alloying elements is important to examine the effect of one alloying element resulting from the interaction of the other element on stacking fault energy. Off-diagonal part of the Table 4.6 shows the binary interactions of all elements. They are obtained from the plane equations of each interaction using *b* and *c* coefficients. On the other hand, diagonal part shows only the effect of one alloying element on SFE. In this way, effect of an alloying element on SFE can be investigated with and without interaction of other elements. Each row indicates the sensitivity values of related alloy.

Table 4.6. All interaction results: Diagonal part is obtained using simple linear regression model and off-diagonal part is obtained using multiple linear regression model

	Cr	*Mn*	*Mo*	*Si*	*Al*	*Cu*	*Co*	*Nb*	*Ni*	*O*	*V*	*B*	*C*
Cr	-0.84	-1.47	-1.63	-2.62	-2.00	-1.77	-2.44	-1.46	-2.55	-1.68	-1.82	-1.38	-0.82
Mn	-0.65	-1.26	-1.34	-1.28	-1.25	-1.23	-1.62	-1.06	-1.87	-1.21	-1.19	-1.35	-0.84
Mo	-1.83	-3.06	-1.71	-4.72	-1.52	-1.96	-4.01	-1.81	-4.61	-1.87	-2.03	-3.72	-3.90
Si	6.00	16.80	15.21	17.64	17.20	17.69	17.00	17.01	15.40	17.71	17.46	15.54	12.08
Al	32.46	35.07	35.88	34.86	35.43	35.59	35.52	34.45	33.94	35.44	35.29	36.28	32.79
Cu	-1.52	1.11	1.13	1.24	1.64	1.41	1.02	1.29	1.81	1.33	1.23	0.84	0.33
Co	2.25	2.95	2.98	3.18	3.29	3.27	3.28	3.33	2.45	3.29	3.21	3.07	3.02
Nb	-3.83	-6.18	-7.03	-7.75	-7.97	-6.93	-6.50	-6.88	-6.85	-6.91	-8.53	-6.01	-6.74
Ni	2.44	2.90	3.02	3.16	3.60	3.66	2.63	3.76	3.82	3.68	3.64	3.00	2.76
O	-6.45	-14.21	-14.7	-12.31	-35.12	-15.21	-14.05	-14.63	-12.65	-13.71	-14.30	-13.39	-10.91
V	-4.18	0.36	-0.70	-1.72	-0.13	0.34	-2.11	-5.30	-0.72	0.48	0.34	0.11	-0.29
B	-122.1	-178.7	-195.1	-212.3	-169.6	-183.8	-201.2	-168.3	-244.5	-181.0	-184.1	-103.1	-137.2
C	36.74	46.72	47.94	57.33	65.99	52.46	46.43	55.26	48.10	52.67	52.42	48.75	52.68

In order to measure how successfully results fit into models, R-squared is used. In this way, it can be learned whether there exists a strong relationship between dependent and independent variables. The results in Table 4.7 gives R-squared values of simple regression models and multiple regression models in diagonal part and off-diagonal part, respectively. According to the results, it can be said that the models possessing R-squared values above 0.8 have good explanatory power and

explain at least 80% of the data. Higher R-squared values indicate that the model fits better and provides more reliable predictions.

Table 4.7. R-squared values for all interactions: Diagonal part is obtained using simple linear regression model and off-diagonal part is obtained using multiple linear regression model.

	Cr	**Mn**	**Mo**	**Si**	**Al**	**Cu**	**Co**	**Nb**	**Ni**	**O**	**V**	**B**	**C**
Cr	0.36	0.66	0.75	0.80	0.87	0.76	0.90	0.69	0.90	0.74	0.78	0.71	0.84
Mn	0.66	0.96	0.95	0.97	0.98	0.95	0.98	0.93	0.95	0.95	0.95	0.96	0.84
Mo	0.75	0.95	1	0.96	1	0.94	0.98	1	0.97	0.97	0.93	0.92	0.96
Si	0.80	0.97	0.96	1	1	1	1	1	0.98	1	1	0.99	0.96
Al	0.87	0.98	1	1	1	1	1	1	1	1	1	1	0.98
Cu	0.76	0.95	0.94	1	1	1	1	1	0.99	1	0.92	0.99	0.97
Co	0.90	0.98	0.98	1	1	1	1	1	0.95	1	1	1	0.95
Nb	0.69	0.93	1	1	1	1	1	1	1	1	0.98	0.99	0.98
Ni	0.90	0.95	0.97	0.98	1	0.99	0.95	1	1	1	1	0.99	0.94
O	0.74	0.95	0.97	1	1	1	1	1	1	0.73	0.69	1	0.97
V	0.78	0.95	0.93	1	1	0.92	1	0.98	1	0.69	0.39	1	0.97
B	0.71	0.96	0.92	0.99	1	0.99	1	0.99	0.99	1	1	1	0.98
C	0.84	0.84	0.96	0.96	0.98	0.97	0.95	0.98	0.94	0.97	0.97	0.98	0.97

When examining the effect of alloying elements on SFE, a group of alloying elements and different wt.% range for each element are considered. Austenitization temperature is critical since it affects the present phases. When stacking fault energy

calculation is performed at 25°C, austenitization temperature is taken as 1100°C and a homogeneous microstructure is desired. GX120Mn steel microstructure has nearly fully austenite phase after austenitization. Alloying elements can cause the formation of new phases at 1100°C besides austenite phase. Therefore, the relationship between SFE and alloying elements may not be linear as expected. It is important for the model to better fit the observed data and for the independent variables to better explain the variance of the dependent variable. In SFE calculations, in addition to the addition of alloying elements changing the SFE, the new phases formed can cause sudden changes in the SFE and disrupt the linearity. This creates a need to use more complex models instead of simpler models. Therefore, in this study, staying in the single phase region as much as possible and using alloying elements whose mass percentage is in a linear relationship with SFE will make the model simpler and stronger.

As depicted in Table 4.7, some R-squared values are below 0.8. A low R-squared value indicates that the model used fails to explain the observed data or that the independent variables are poor at explaining the variance of the dependent variable. This may indicate that the predictive ability of the model is low and the independent variables used are insufficient to explain the dependent variable.

If the calculations are made in wt.% ranges where there is a single phase, there are no sudden changes in SFE and the R-squared value is very close to 1, meaning it fits the model very well. On the other hand, at percentage values where SFE suddenly changes, that is, where it goes out of linearity, a new phase usually forms, for example a liquid phase or carbide is formed. In this case, we can say that if the current phase was preserved, linearity could also be preserved. For example, in Cr-V interaction, SFE linearly increases as wt.% of V increases from 0 wt.% to 0.45 wt.%. Beyond 0.45 wt.%, SFE decreases due to the possible effect of carbide formation. Therefore, using the linear part is important for the model to provide a better fit and more reliable predictions.

Although the formation of different phases (liquid phase, carbides) at the austenitization temperature with the addition of new alloying elements or changing the amounts of existing elements disrupts the linear relationship between the weight percentage of alloying elements and SFE, the regression analysis shows that the model is mostly suitable. Therefore, it can be seen that the applied models generally have a high R-squared value and are therefore statistically significant.

Figure 4.7 to 4.19 compare the sensitivity parameter of Cr, Mn, Mo, Si, Al, Cu, Co, Nb, Ni, O, V, B and C with and without interaction with other elements. The red dashed line in the given bar chart represents the sensitivity of the element alone. The other bars show the element sensitivity when interacting with different elements.

When there are significant differences between the sensitivity value of an element alone, shown in the red dashed line, and the height of the other bars, then the sensitivity of the element when interacting with other elements changes significantly. The sensitivity of the element increases when interacting with some elements, while with others it may decrease or remain almost unchanged. This comparison is valuable for understanding how this element responds in different conditions and may help determine which interactions are more prominent.

The cases where there is a larger difference between the bars indicate that the sensitivity of the element changes more when it interacts with other elements. Therefore, it can be concluded that as the height of the bars increases or decreases, the corresponding element affects the sensitivity more noticeably.

According to the Figure 4.2, with the exception of Cr, SFE varies linearly or nearly linearly depending on the weight percent values of the other elements. For Cr element, SFE increases with increasing of Cr amount up to about 6 wt.%, then, decreases with increasing of Cr amount. Therefore, this non-linear relationship negatively affects the sensitivity analysis. The R-squared values for Cr in Table 4.7 also support this.

When examining Figure 4.7 to Figure 4.19, the following inferences can be made, respectively:

- Sensitivity of Cr is mainly affected by Si, Co, Ni. When Cr is used together with these elements, it has a greater lowering effect on SFE.
- While Ni and Co further increase the SFE-lowering effect of Mn, Cr further reduces the SFE-lowering effect of Mn.
- While Mn, Si, Co, Ni, B, and C elements increase the SFE-lowering effect of Mo, the presence of other elements almost does not affect the sensitivity of Mo.
- While Cr and C elements significantly reduce the SFE-enhancing effect of Si, the presence of other elements almost does not affect the sensitivity of Si.
- The presence of other elements almost does not affect the sensitivity of Al.
- While the elements Cr, B, and C significantly reduce the SFE-enhancing effect of Cu, the presence of Cr changes the sensitivity of Cu from positive to negative.
- Cr and Ni elements reduce the SFE-increasing effect of Co.
- While the V element enhances the SFE-reducing effect of Nb, the presence of the Cr element diminishes this effect.
- Elements other than Al, Cu, Nb, O, and V diminish the SFE-increasing effect of Ni.
- While the Cr element reduces the SFE-reducing effect of O, the presence of the Al element significantly increases the SFE-reducing effect of O.
- Cr, Si, Co and Nb elements give V a SFE-reducing effect.
- Alloying elements, especially Ni, generally enhance the SFE-reducing effect of B.
- While the Cr element reduces the SFE-increasing effect of C, the presence of the Al element increases the SFE-increasing effect of C.

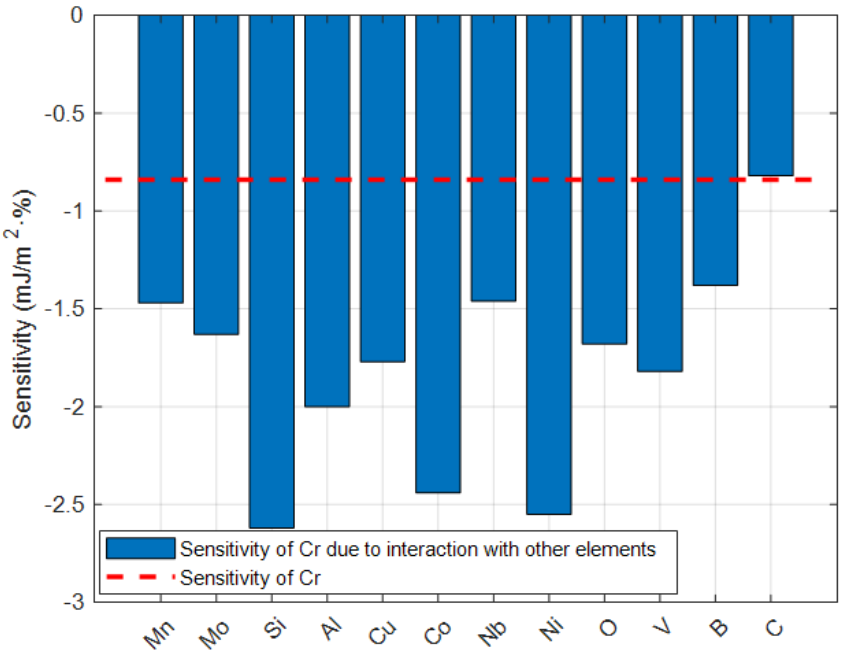

Figure 4.7. Sensitivity of Cr with and without interaction with other elements.

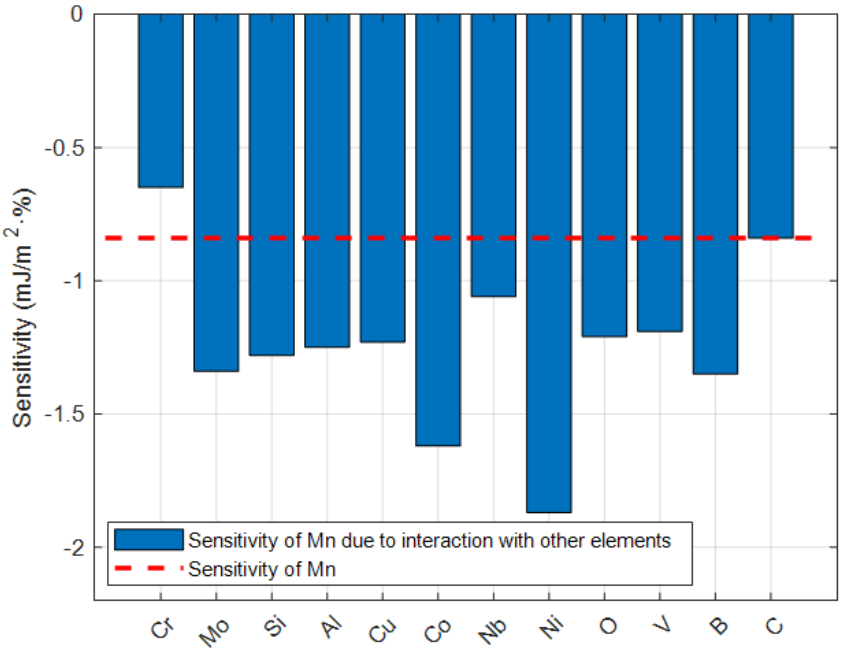

Figure 4.8. Sensitivity of Mn with and without interaction with other elements.

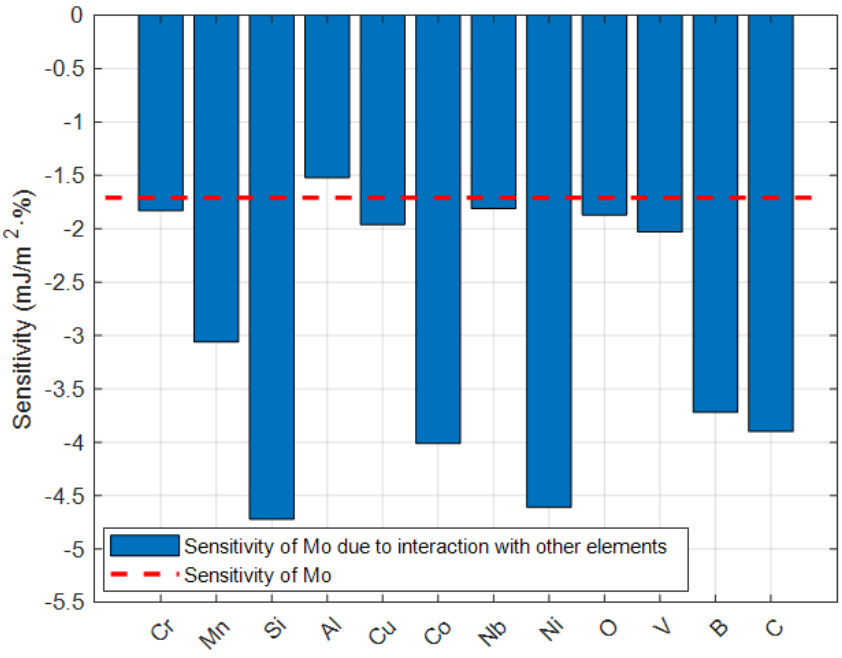

Figure 4.9. Sensitivity of Mo with and without interaction with other elements.

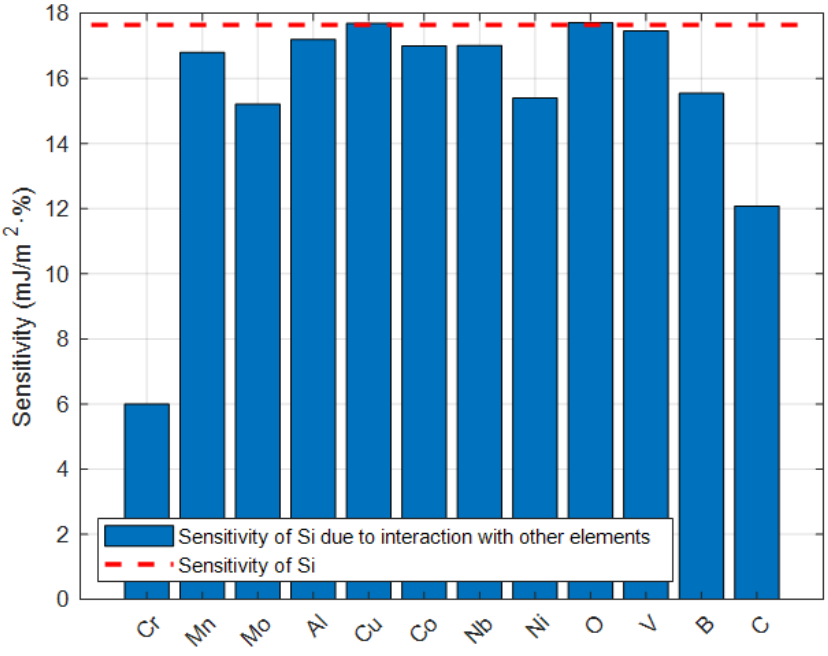

Figure 4.10. Sensitivity of Si with and without interaction with other elements.

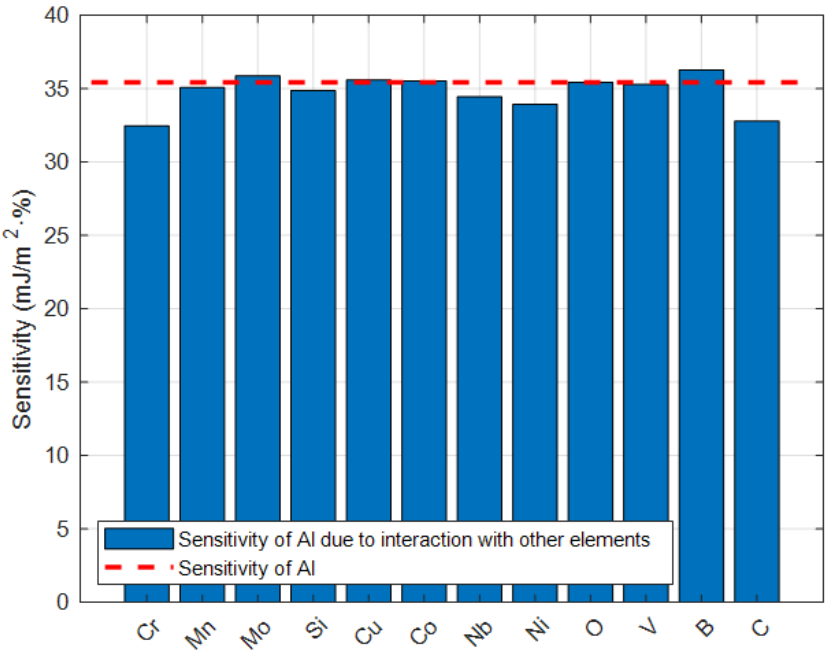

Figure 4.11. Sensitivity of Al with and without interaction with other elements.

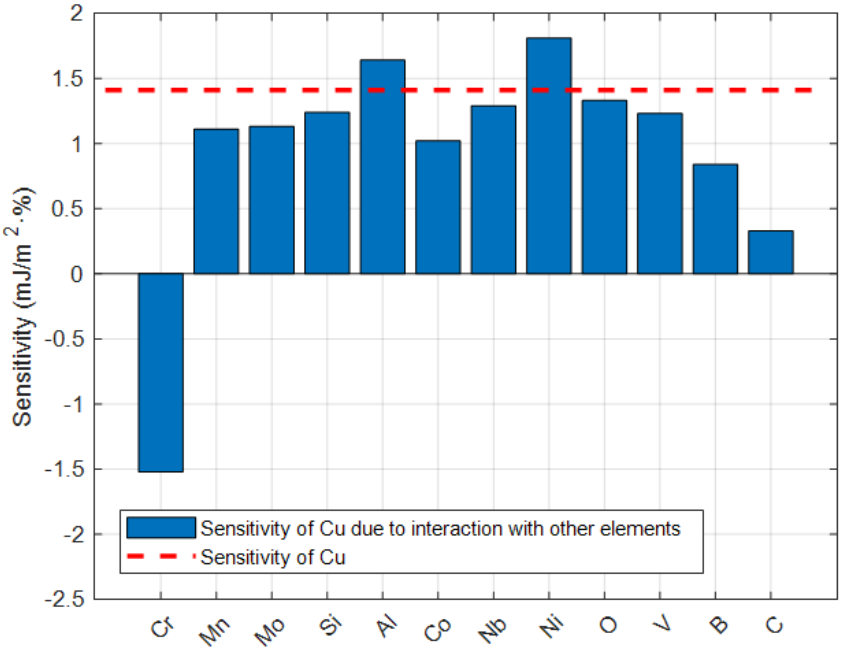

Figure 4.12. Sensitivity of Cu with and without interaction with other elements.

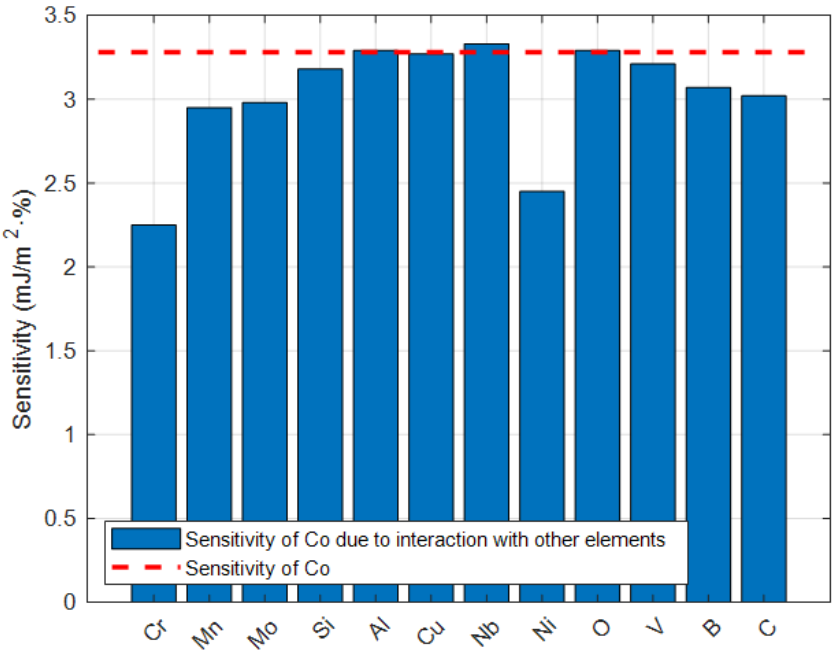

Figure 4.13. Sensitivity of Co with and without interaction with other elements.

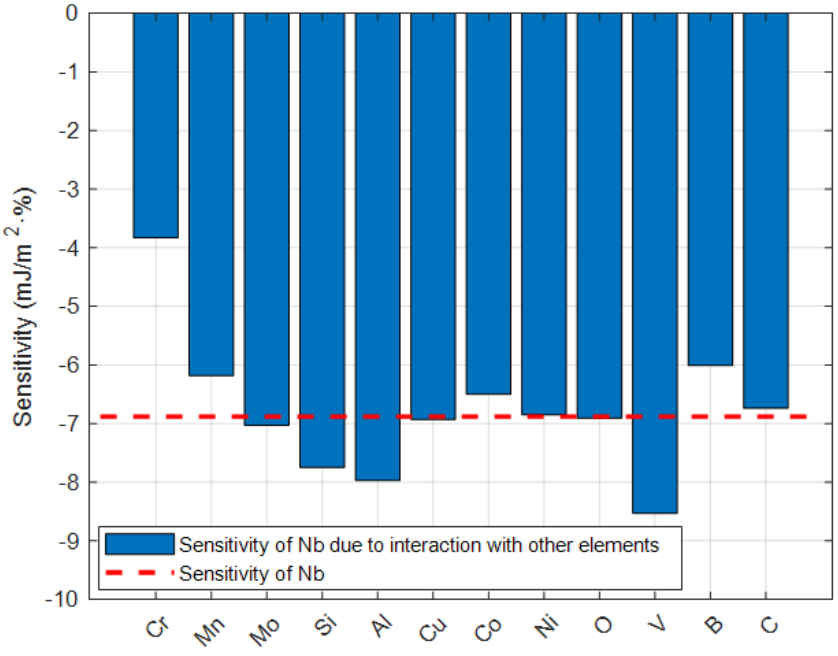

Figure 4.14. Sensitivity of Nb with and without interaction with other elements.

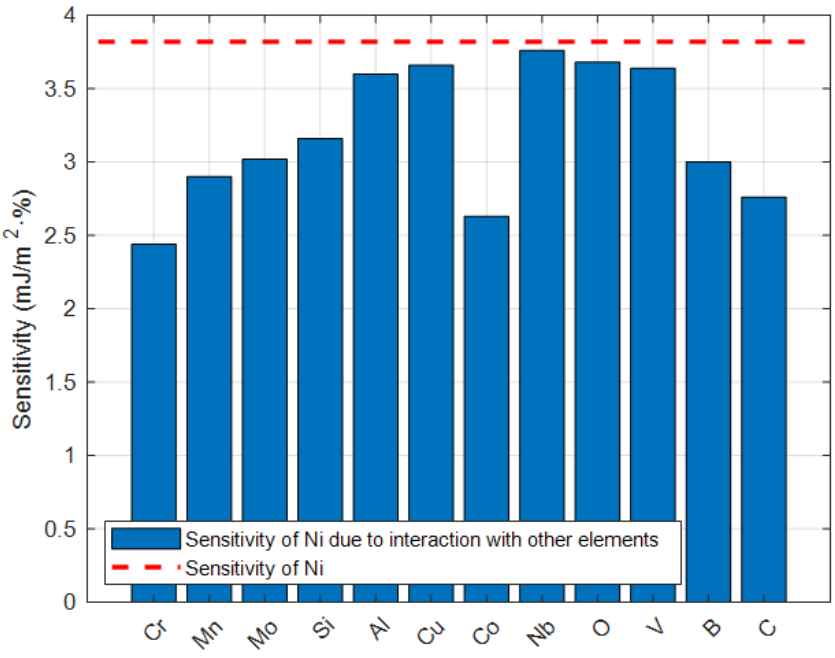

Figure 4.15. Sensitivity of Ni with and without interaction with other elements.

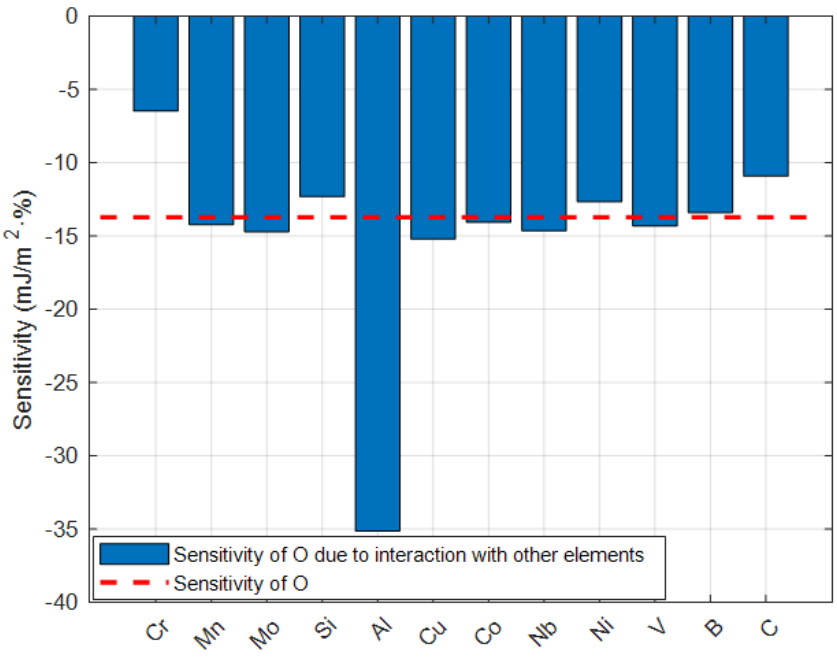

Figure 4.16. Sensitivity of O with and without interaction with other elements.

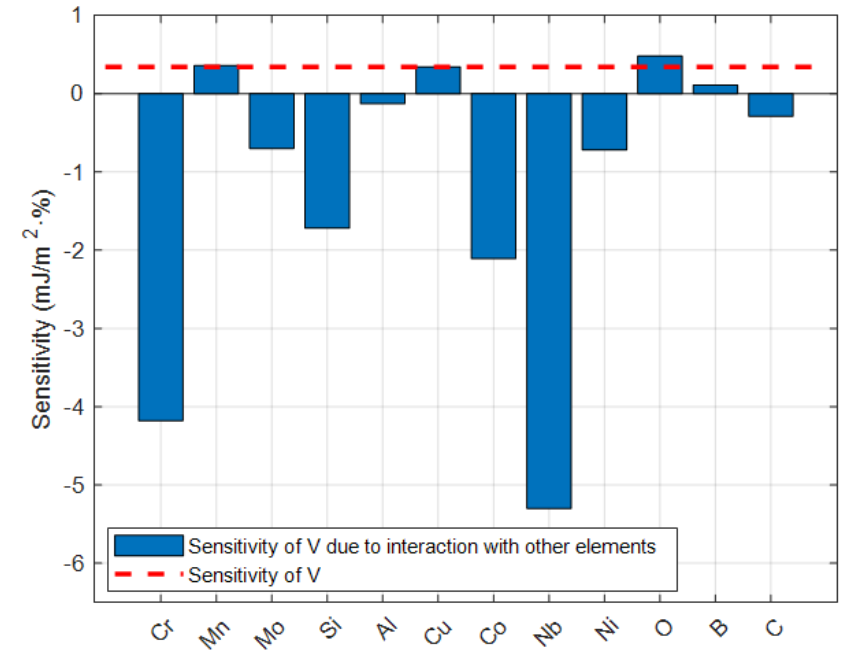

Figure 4.17. Sensitivity of V with and without interaction with other elements.

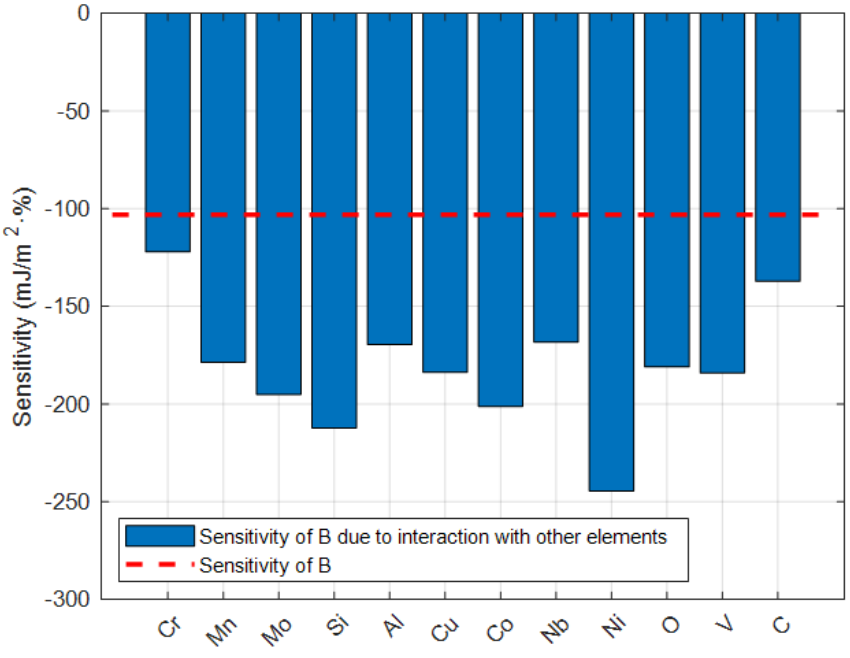

Figure 4.18. Sensitivity of B with and without interaction with other elements.

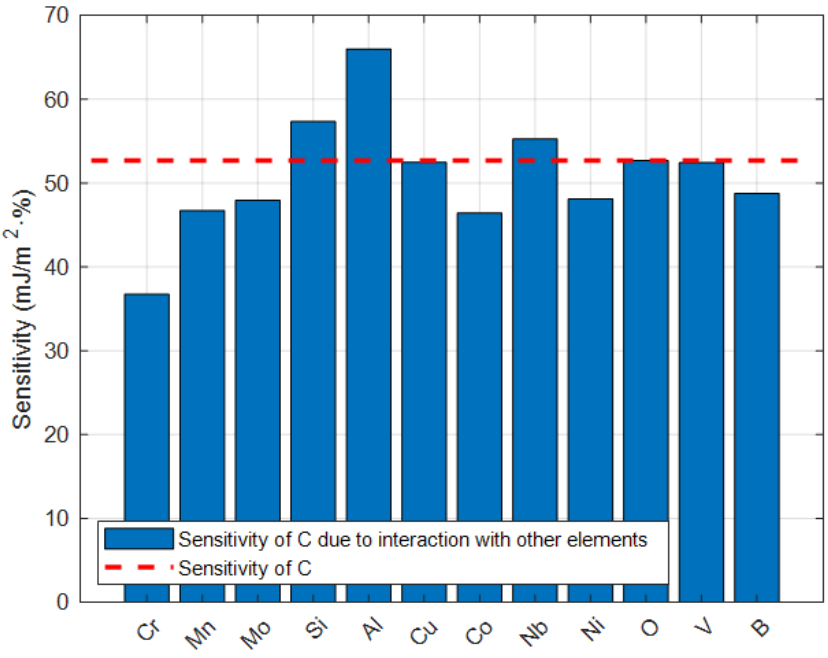

Figure 4.19. Sensitivity of C with and without interaction with other elements.

For this study, *interaction terms* are also added to regression analysis because it is likely that there is an interaction between the independent variables in the model. That is, there is a joint effect of two different alloying elements on the SFE. In order to examine that the relationship between SFE and wt.% of an alloy is affected by another wt.% of another alloy, a linear regression model with an interaction term is used. In modeling the stacking fault energy (y), two features are used: wt.% of alloy A (x_1) and wt.% of alloy B (x_2). In order to obtain the coefficients, data is gathered and a linear regression model with an interaction term is estimated according to the following equation.

$$y = a + b\,x_1 + c\,x_2 + d\,x_1\,x_2$$

The coefficient d represents the interaction between x_1 and x_2. Thus, the relationship between the variables x_1 and x_2 can be represented in the model in a non-linear manner.

Off-diagonal part of the Table 4.8 shows the coefficients of interaction terms for 2-combinations of 13 alloying elements. They are obtained from the multiple linear regression model with interaction terms using *d* coefficients. On the other hand, diagonal part is not applicable (NA) since there are no interaction terms due to simple linear model. The magnitude and sign of the coefficient of the interaction term gives an idea about the sensitivity of the interaction. Therefore, each cell in the table indicates the sensitivity of interactions.

Table 4.8. The coefficients of interaction terms (Diagonal part is not applicable (NA) due to the simple linear regression model.)

	Cr	**Mn**	**Mo**	**Si**	**Al**	**Cu**	**Co**	**Nb**	**Ni**	**O**	**V**	**B**	**C**
Cr	NA	0.11	0.06	-1.54	-0.63	-0.40	-0.14	0.45	-0.15	1.04	-0.49	11.43	-2.72
Mn	0.11	NA	-0.21	-0.13	-0.09	-0.06	-0.09	0.32	-0.15	0.07	0.12	-1.43	-2.94
Mo	0.06	-0.21	NA	-4.10	0.46	-0.47	-0.49	-0.09	-0.60	-0.50	-1.19	10.56	-4.58
Si	-1.54	-0.13	-4.10	NA	-1.09	-0.14	-0.21	-1.42	-0.80	-1.65	-3.31	-70.17	7.93
Al	-0.63	-0.09	0.46	-1.09	NA	0.58	-0.01	-2.06	-0.24	-10.74	-1.30	23.42	26.12
Cu	-0.40	-0.06	-0.47	-0.14	0.58	NA	-0.06	-0.09	-0.05	0.25	-0.65	-12.55	-1.20
Co	-0.14	-0.09	-0.49	-0.21	-0.01	-0.06	NA	0.08	-0.22	0.18	-0.54	-3.87	-1.19
Nb	0.45	0.32	-0.09	-1.42	-2.06	-0.09	0.08	NA	0.10	3.80	-6.34	25.67	5.04
Ni	-0.15	-0.15	-0.60	-0.80	-0.24	-0.05	-0.22	0.10	NA	0.84	-0.23	-11.73	-0.95
O	1.04	0.07	-0.50	-1.65	-10.74	0.25	0.18	3.80	0.84	NA	1.65	8.27	-4.84
V	-0.49	0.12	-1.19	-3.31	-1.30	-0.65	-0.54	-6.34	-0.23	1.65	NA	-13.36	-1.07
B	11.43	-1.43	10.56	-70.17	23.42	-12.55	-3.87	25.67	-11.73	8.27	-13.36	NA	-111.4
C	-2.72	-2.94	-4.58	7.93	26.12	-1.20	-1.19	5.04	-0.95	-4.84	-1.07	-111.4	NA

Figure 4.20 shows the heat map of Table 4.8 containing the coefficients of interaction terms for the regression model. This map provides a visual representation of the values. To comment the table and figure, it is important to understand what the values in each cell represent. Each cell contains the coefficient of the interaction term of the corresponding two different elements. For example, the value in the second column of the first row is the coefficient by which the Cr interacts with the Mn. In this model, the coefficients of the interaction terms determine the sensitivity of the interaction between the variables of interest. For example, a positive coefficient may indicate that the interaction between the independent variables of interest has a positive effect on the dependent variable, while a negative coefficient may indicate that the interaction has a negative effect on the dependent variable. It can be seen from Figure 4.20; Al-B, Al-C and Nb-B show great interactions. On the other hand, C-B and Si-B have small interactions. High coefficients in interaction terms may indicate that the SFE responds more sensitively to the interaction between the alloys interest. This means that the value of the SFE is more sensitive to changes in the interaction terms that represent the relationship between the alloys interest. Therefore, when interpreting the results, it is important to consider which interaction between variables each interaction term represents and the effect of this interaction on the model results. This type of analysis can be an important tool for understanding complex relationships between variables and assessing model accuracy.

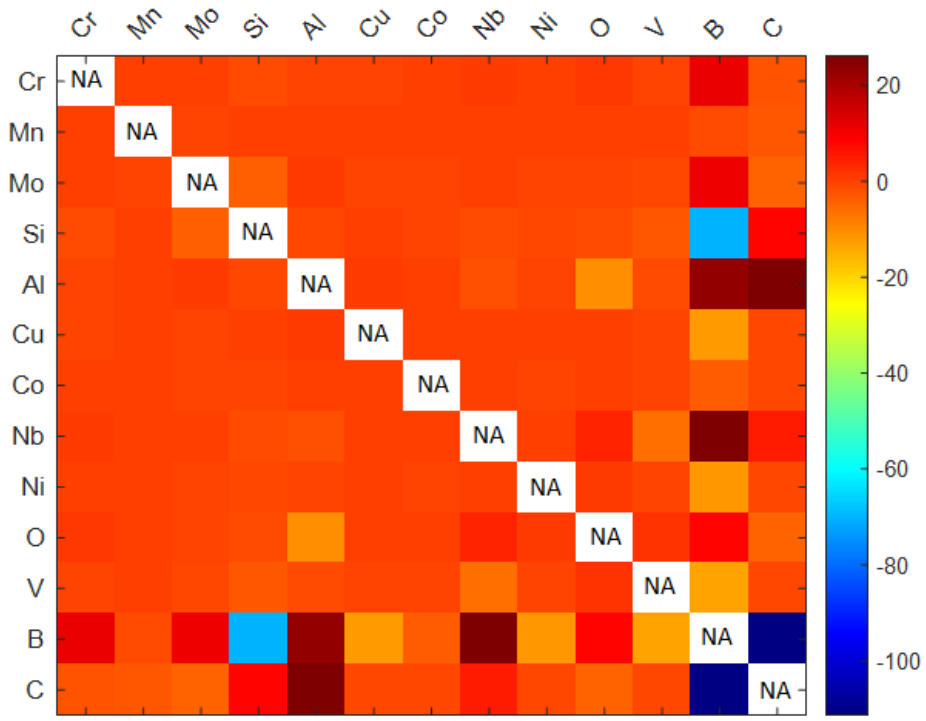

Figure 4.20. The heat map of the coefficients of interaction terms

Considering all the calculations and analyses performed, it can be said that linear regression model is a powerful tool used to understand the relationship between SFE and wt.% of alloying elements. Also, sensitivity analysis provides understanding the behavior of model, determining the importance of input variables and evaluating the reliability of model. Thus, this analysis can be used for many other different purposes, such as, understanding the effects of alloying elements on martensitic transformation temperatures (Ms, Md(50/30)). In this way, reliable predictions can be made using models obtained with accurate and high-quality data.

CHAPTER 5

CONCLUSION

In this study, the effect of alloying elements on critical martensitic transformation parameterss (temperatures and stacking fault energy) in austenitic manganese steels is examined usingcomputational methods. Stacking fault energy (SFE), martensite transformation temperatures (Ms and Md(50/30)) are calculated using JMatProwhile Thermo-Calc is used to calculate T-Zero temperatures and Ms temperatures for comparison.

According to the results obtained by using simple linear regression model, addition of elements that reduce SFE, such as Nb, B and O, can increase the tendency of deformation-induced martensite formation at near ambient temperatures. In order to keep the M_S temperature at a low level (to avoid thermal martensite formation), the amount of Mn should not be reduced too much below the standard. Among the elements examined, Co appears to be the only element that increases the Md temperature. It also raises the T-Zero temperature significantly. Therefore, it can be said that the Co element positively affects the martensite transformation due to deformation. In addition, Cr, Mo and O also increase the T-Zero temperature.

According to the results obtained by using multiple linear regression model, all the calculations and analyses conducted suggest that the linear regression model serves as a potent tool for comprehending the correlation between SFE and the weight percentage of alloying elements. Considering the effects of the interactions of element pairs on SFE; it has been observed that the coefficient values of the interaction terms of Al-B, Al-C and Nb-B element pairs are relatively larger. This means that these pairs of elements, when combined, have a significant and strong increasing effect on SFE. The higher interaction coefficients between these pairs indicate that the SFE responds more sensitively with the combined use of these

elements. This implies that the value of SFE is more sensitive to the change of combinations of these elements. On the other hand, it is observed that the coefficient values of the interaction terms of C-B and Si-B element pairs are relatively smaller. This means that these pairs of elements, when combined, have a significant and strong decreasing effect on SFE. The lower interaction coefficients between these pairs indicate that SFE responds more sensitively but negatively to the combined use of these elements.

In future, as the study already contains a large amount of data, the data can further be analyzed and processed by other statistical techniques. Then processed data can be used to design a new alloy. On the other hand, it is more important to conduct some experimental studies for the validation of simulation results before proceeding with an alloy design.

REFERENCES

[1] Y.N. Dastur, W.C. Leslie, Mechanism of Work Hardening in Hadfield Manganese Steel, Metall. Trans. A, Phys. Metall. Mater. Sci. 12 A (1981) 749–759. https://doi.org/10.1007/BF02648339.

[2] P. Chowdhury, D. Canadinc, H. Sehitoglu, On deformation behavior of Fe-Mn based structural alloys, Mater. Sci. Eng. R Reports. 122 (2017) 1–28. https://doi.org/10.1016/J.MSER.2017.09.002.

[3] P.H. Adler, G.B. Olson, W.S. Owen, Strain Hardening of Hadfield Manganese Steel, (n.d.).

[4] I. Karaman, H. Sehitoglu, A.J. Beaudoev, Y.I. Chumlyakov, H.J. Maier, C.N. Tomé, Modeling the deformation behavior of Hadfield steel single and polycrystals due to twinning and slip, Acta Mater. 48 (2000) 2031–2047. https://doi.org/10.1016/S1359-6454(00)00051-3.

[5] W.S. Owen, M. Grujicic, Strain aging of austenitic Hadfield manganese steel, Acta Mater. 47 (1998) 111–126. https://doi.org/10.1016/S1359-6454(98)00347-4.

[6] C. Efstathiou, H. Sehitoglu, Strengthening Hadfield steel welds by nitrogen alloying, Mater. Sci. Eng. A. 506 (2009) 174–179. https://doi.org/10.1016/J.MSEA.2008.11.057.

[7] ASTM-A128/A128M-93, Standard Specification for Steel Castings, Austentic Manganese, ASTM Int. West Conshohocken, PA, USA. (2017). https://doi.org/10.1520/A0128.

[8] T. Materials, ASM Metals HandBook Volume 1 - Properties and Selections - Irons Steels and High and Performance, Technology. 2 (2001) 3470. http://books.google.com.hk/books?id=eC-Zt1J4oCgC.

[9] B. Sun, A. Kwiatkowski da Silva, Y. Wu, Y. Ma, H. Chen, C. Scott, D. Ponge, D. Raabe, Physical metallurgy of medium-Mn advanced high-strength steels, Int. Mater. Rev. 68 (2023) 786–824. https://doi.org/10.1080/09506608.2022.2153220.

[10] B. Sun, F. Fazeli, C. Scott, B. Guo, C. Aranas, X. Chu, M. Jahazi, S. Yue, Microstructural characteristics and tensile behavior of medium manganese steels with different manganese additions, (2018). https://doi.org/10.1016/j.msea.2018.04.115.

[11] M. Palumbo, Thermodynamics of martensitic transformations in the framework of the CALPHAD approach, Calphad. 32 (2008) 693–708. https://doi.org/10.1016/J.CALPHAD.2008.08.006.

[12] G.B. Olson, M. Cohen, A mechanism for the strain-induced nucleation of martensitic transformations, J. Less-Common Met. 28 (1972) 107–118.

[13] H.W. Yen, S.W. Ooi, M. Eizadjou, A. Breen, C.Y. Huang, H.K.D.H. Bhadeshia, S.P. Ringer, Role of stress-assisted martensite in the design of strong ultrafine-grained duplex steels, Acta Mater. 82 (2015) 100–114. https://doi.org/10.1016/J.ACTAMAT.2014.09.017.

[14] P.J. Gibbs, B.C. De Cooman, D.W. Brown, B. Clausen, J.G. Schroth, M.J. Merwin, D.K. Matlock, Strain partitioning in ultra-fine grained medium-manganese transformation induced plasticity steel, Mater. Sci. Eng. A. 609 (2014) 323–333. https://doi.org/10.1016/J.MSEA.2014.03.120.

[15] D.M. Field, L.G. Garza-Martinez, D.C. Van Aken, Processing and Properties of Medium-Mn TRIP Steel to Obtain a Two-Stage TRIP Behavior, Metall. Mater. Trans. A Phys. Metall. Mater. Sci. 51 (2020) 4427–4433. https://doi.org/10.1007/S11661-020-05901-2/TABLES/5.

[16] I. Tamura, Deformation-induced martensitic transformation and transformation-induced plasticity in steels, Met. Sci. 16 (1982) 245–253. https://doi.org/10.1179/030634582790427316.

[17] P. Hedström, Deformation and Martensitic Phase Transformation in Stainless Steels, Luleå Univ. Technol. (2007).

[18] T. Angel, Formation of Martensite in Austenitic Stainless Steel, J. Iron Steel Inst. 177 (1954) 165–174. http://ci.nii.ac.jp/naid/10026799705/en/ (accessed August 19, 2021).

[19] Z. Pei, An overview of modeling the stacking faults in lightweight and high-entropy alloys: Theory and application, Mater. Sci. Eng. A. 737 (2018) 132–150. https://doi.org/10.1016/j.msea.2018.09.028.

[20] R. Allende-Seco, A. Artigas, H. Bruna, L. Carvajal, A. Monsalve, M.F. Sklate-Boja, Hardening by transformation and cold working in a hadfield steel cone crusher liner, Metals (Basel). 11 (2021) 961. https://doi.org/10.3390/met11060961.

[21] W. Woo, J.S. Jeong, D.-K. Kim, C.M. Lee, S.-H. Choi, J.-Y. Suh, S.Y. Lee, S. Harjo, T. Kawasaki, Stacking Fault Energy Analyses of Additively Manufactured Stainless Steel 316L and CrCoNi Medium Entropy Alloy Using In Situ Neutron Diffraction, Sci. Reports 2020 101. 10 (2020) 1–15. https://doi.org/10.1038/s41598-020-58273-3.

[22] J.K. Kim, B.C. De Cooman, Stacking fault energy and deformation mechanisms in Fe-xMn-0.6C-yAl TWIP steel, Mater. Sci. Eng. A. 676 (2016) 216–231. https://doi.org/10.1016/j.msea.2016.08.106.

[23] S. Allain, J.P. Chateau, O. Bouaziz, S. Migot, N. Guelton, Correlations between the calculated stacking fault energy and the plasticity mechanisms in Fe-Mn-C alloys, Mater. Sci. Eng. A. 387–389 (2004) 158–162. https://doi.org/10.1016/j.msea.2004.01.059.

[24] B.K. Zuidema, D.K. Subramanyam, W.C. Leslie, The Effect of Aluminum on the Work Hardening and Wear Resistance of Hadfield Manganese Steel, Metall. Trans. A, Phys. Metall. Mater. Sci. 18 A (1987) 1629–1639. https://doi.org/10.1007/BF02646146.

[25] Y.K. Lee, C.S. Choi, Driving force for γ → ε martensitic transformation and stacking fault energy of γ in Fe-Mn binary system, Metall. Mater. Trans. A Phys. Metall. Mater. Sci. 31 (2000) 355–360. https://doi.org/10.1007/s11661-000-0271-3.

[26] B.C. De Cooman, High Mn TWIP steel and medium Mn steel, (2017). https://doi.org/10.1016/B978-0-08-100638-2.00011-0.

[27] P.J. Gibbs, E. De Moor, M.J. Merwin, B. Clausen, J.G. Speer, D.K. Matlock, Austenite stability effects on tensile behavior of manganese-enriched-austenite transformation-induced plasticity steel, Metall. Mater. Trans. A Phys. Metall. Mater. Sci. 42 (2011) 3691–3702. https://doi.org/10.1007/S11661-011-0687-Y/FIGURES/12.

[28] Y. Ma, B. Sun, A. Schökel, W. Song, D. Ponge, D. Raabe, W. Bleck, Phase boundary segregation-induced strengthening and discontinuous yielding in ultrafine-grained duplex medium-Mn steels, Acta Mater. 200 (2020) 389–403. https://doi.org/10.1016/J.ACTAMAT.2020.09.007.

[29] A. Saeed-Akbari, J. Imlau, U. Prahl, W. Bleck, Derivation and Variation in Composition-Dependent Stacking Fault Energy Maps Based on Subregular Solution Model in High-Manganese Steels, (n.d.). https://doi.org/10.1007/s11661-009-0050-8.

[30] G.R. Lehnhoff, K.O. Findley, B.C. De Cooman, The influence of silicon and aluminum alloying on the lattice parameter and stacking fault energy of austenitic steel, Scr. Mater. 92 (2014) 19–22. https://doi.org/10.1016/J.SCRIPTAMAT.2014.07.019.

[31] A. Dumay, J.P. Chateau, S. Allain, S. Migot, O. Bouaziz, Influence of addition elements on the stacking-fault energy and mechanical properties of an austenitic Fe-Mn-C steel, Mater. Sci. Eng. A. 483–484 (2008) 184–187. https://doi.org/10.1016/j.msea.2006.12.170.

[32] U.S. Anamu, O.O. Ayodele, E. Olorundaisi, B.J. Babalola, P.I. Odetola, A.

Ogunmefun, K. Ukoba, T.C. Jen, P.A. Olubambi, Fundamental design strategies for advancing the development of high entropy alloys for thermo-mechanical application: A critical review, J. Mater. Res. Technol. 27 (2023) 4833–4860. https://doi.org/10.1016/J.JMRT.2023.11.008.

[33] S.C. Chapra, Applied Numerical Methods With MATLAB for Engineers and Scientists, 2002.

[34] V.A. Barbur, D.C. Montgomery, E.A. Peck, Introduction to Linear Regression Analysis., 1994. https://doi.org/10.2307/2348362.

[35] B.P. Maradit, Analytical, Numerical And Experimental Investigation Of The Distortion Behavior Of Steel Shafts During Through-Hardening, 2010.

[36] A. Saltelli, S. Tarantola, F. Campolongo, M. Ratto, Sensitivity analysis in practice: a guide to assessing scientific models (Google eBook), 2004. http://books.google.com/books?id=NsAVmohPNpQC&pgis=1f.

[37] J. Kim, B.C. De Cooman, On the stacking fault energy of Fe-18 pct Mn-0.6 pct C-1.5 pct Al twinning-induced plasticity steel, Metall. Mater. Trans. A Phys. Metall. Mater. Sci. 42 (2011) 932–936. https://doi.org/10.1007/S11661-011-0610-6.